Design of an ACIM Vector Control Drive using the 56F8013 Device

Designer Reference Manual

56800E
16-bit Digital Signal Controllers

DRM075
Rev 1
11/2005

freescale.com

freescale semiconductor

Design of an ACIM Vector Control Drive using the 56F8013 Device

Designer Reference Manual

To provide the most up-to-date information, the revision of our documents on the World Wide Web will be the most current. Your printed copy may be an earlier revision. To verify that you have the latest information available, refer to http://www.freescale.com

The following revision history table summarizes changes contained in this document. For your convenience, the page number designators have been linked to the appropriate location.

Revision History

Date	Revision Level	Description	Page Number(s)
10/2005	0	Initial release	N/A
11/2005	1	Corrected term “Intelligent Power Module” to “Integrated Power Module”	xi, 3-3

TABLE OF CONTENTS

Chapter 6
Hardware Implementation

Chapter 7
Software Design

Chapter 8
JTAG Simulation and SCI Communication

Chapter 9
Operation

LIST OF FIGURES

LIST OF TABLES

About This Document

This manual describes the use of a 56F8013 device in an ACIM Vector Control Drive application.

Audience

This manual targets design engineers interested in developing an ACIM Vector Control Drive application.

Organization

This User's Manual consists of the following sections:

- **Chapter 1, Introduction,** explains how an AC Induction Motor and a 56F8013 device facilitate a vector control drive design.
- **Chapter 2, Benefits and Features of the 56F8013 Controller,** highlights the advantages in using a 56F8013 controller.
- **Chapter 3, Motor Drive System,** details the features and design of a motor drive system.
- **Chapter 4, ACIM Theory,** describes software, control and configuration of an AC Induction Motor.
- **Chapter 5, Design Concept of an ACIM Vector Control Drive,** details the design concept of an AC Induction Motor vector control drive.
- **Chapter 6, Hardware Implementation,** describes how to set up the hardware needed for a vector control drive application.
- **Chapter 7, Software Design,** explains the software system design.
- **Chapter 8, JTAG Simulation and SCI Communication,** describes the application's debugging and communications functions.
- **Chapter 9, Operation,** explains how to use the application.
- **Appendix A, Schematics,** contains schematics for the ACIM vector control drive application.
- **Appendix B, ACIM Bill of Materials,** lists all parts used in the application.

Conventions

This document uses the following notational conventions:

Typeface, Symbol or Term	Meaning	Examples
`Courier Monospaced Type`	Code examples	`//Process command for line flash`
Italic	Directory names, project names, calls, functions, statements, procedures, routines, arguments, file names, applications, variables, directives, code snippets in text	...and contains these core directories: *applications* contains applications software... ...CodeWarrior project, *3des.mcp* is... ...the *pConfig* argument.... ...defined in the C header file, *aec.h*....
Bold	Reference sources, paths, emphasis	...refer to the **Targeting DSP56F83xx Platform** manual.... ...see: **C:\Program Files\Freescale\help\tutorials**
Blue Text	Linkable on-line	...refer to Chapter 7, License....
Number	Any number is considered a positive value, unless preceded by a minus symbol to signify a negative value	3V -10 DES^{-1}
ALL CAPITAL LETTERS	# defines/ defined constants	# define INCLUDE_STACK_CHECK
Brackets [...]	Function keys	...by pressing function key [F7]
Quotation marks, "..."	Returned messages	...the message, "Test Passed" is displayed.... ...if unsuccessful for any reason, it will return "NULL"...

Definitions, Acronyms, and Abbreviations

The following list defines the acronyms and abbreviations used in this document. As this template develops, this list will be generated from the document. As we develop more group resources, these acronyms will be easily defined from a common acronym dictionary. Please note that while the acronyms are in solid caps, terms in the definition should be initial capped ONLY IF they are trademarked names or proper nouns.

ACIM	Alternating Current Induction Motor
ADC	Analog-to-Digital Conversion
COP	Computer Operating Properly
DCM	Discontinuous Current Mode
EMF	Electro-Magnetic Force
EVM	Evaluation Module
GPIO	General Purpose Input/Output
HMI	Human Machine Interface
I^2C or I2C	Inter-Integrated Circuit
IC	Integrated Circuit
IM	Induction Motor
IPM	Integrated Power Module
ISR	Interrupt Service Routine
LPF	Low-Pass Filter
PFC	Power Factor Correction
PI	Proportional-Integral
PLL	Phase Locked Loop
PWM	Pulse Width Modulation or Modulator
RMS	Root Mean Square
SCI	Serial Communication Interface
SFOC	Stator-Flux-Oriented Control
SPI	Serial Peripheral Interface
SV	Space Vector
SVPWM	Space Vector Pulse Width Modulation

References

The following sources were used to produce this book; we recommend that you have a copy of these references:

1. *DSP56800E Reference Manual,* DSP56800ERM, Freescale Semiconductor, Inc.
2. *56F8000 Peripheral User Manual*, MC56F8000RM, Freescale Semiconductor, Inc.
3. *56F8013 Data Sheet*, MC56F8013, Freescale Semiconductor, Inc.
4. *Inside Code Warrior*
5. X.Xu, R.De Donker, and D.W.Novonty, “A Stator Flux Oriented Induction Machine Drive”, in PESC 1988 Conf.Rec. pp.870-876.
6. C.J.Francis,H.Z.de la Parra, and K.W.E.Cheng, “Practical Implementation of a Stator Flux Oriented Control Scheme for an Induction Machine,” in Power Electronics and Variable-speed Drives, October 1994, pp.54-59
7. J.O.Pinto,B.K.Bose, and L.E.B.da Silva, “A Stator-Flux-Oriented Vector-Controlled Induction Motor Drive with Space-Vector PWM and Flux-Vector Synthesis by Neural Networks,” IEEE Trans. Ind. Appli.,vol.37, no.5,pp.1308-1318. Sep. 2001.
8. M.H.Shin, D.S.Hyun, and S.B.Cho, “Maximum Torque Control of Stator-Flux-Oriented Induction Machine Drive in the Field-Weakening Region,” IEEE Trans Ind. Appli. vol.38,no.1,pp.117-122,Jan.2002.
9. Y.Ruan, X.H.Zhang, J.Xu and etc. “Stator Flux Oriented Control of Induction Motors,” Tans. Of China Electro.Society, vol.18, no.2, pp.1-4, Apr.2003.
10. Yonghong Xue, Xingyi Xu, and T.G.Habelter, “A Stator Flux-Oriented Voltage Source Variable-Speed Drive Based on DC Link Measurement,” IEEE Tran. Ind.Appl. vol.27, no.5, pp.962-969, Sep.1991.
11. Jie Chen,Yongdong Li, and Wei Dong, “A Novel Stator-Flux-Oriented Speed Sensorless Induction Motor Control System using Flux Tracking Strategy,” in Inter.Conf. On Power Elec. And Drive System, PEDS’99, Hong Kong, pp.609-614.
12. Ju-Suk.Lee, T.Takeshita, and N.Matsui, “Stator-Flux-Oriented Sensorless Induction Motor Drive for Optimum Low-Speed Performance,” IEEE Tran. Ind. Appli. vol.33,no.5,pp.1170-1176, Sep.1997.
13. L.Ben-Brahim and A.Kawamura, “A Fully Digitized Field-Oriented Controlled Induction Motor Drive using Only Current Sensors,” IEEE Trans. Ind. Electro.,vol.39,pp.241-249, June 1992.
14. Jun Hu, and Bin Wu, “New Integration Algorithms for Estimating Motor Flux over a Wide Speed Range,” IEEE Trans. on Power Electronics, vol.13, no.5, pp.969-977, Sep.1998.
15. N.R.N.Idris, and A.H.M Yatim, “An Improved Stator Flux Estimation in Steady-State Operation for Direct Torque Control of Induction Machines,” IEEE Trans. Ind.Appl., vol.38, no.1, pp.110-116, Jan.2002.
16. *3-Phase AC Induction Motor Vector Control using a 56F80x, 56F8100 or 56F8300 Device Design of Motor Control Application*, Freescale Semiconductor, Inc., 2004
17. *3-Phase AC Motor Control with VHz Speed Close Loop using the 56F80x*, Freescale Semiconductor, Inc., 2001

Chapter 1 Introduction

1.1 Introduction

This drive application allows vector control of an AC Induction Motor (ACIM) running in a closed-speed loop without a speed/position sensor coupled to the shaft. The application serves as an example of AC induction vector control drive design using a Freescale 56F8013 with Processor Expert^{TM} (PE) software support.

AC induction motors, which contain a cage, are very popular in variable-speed drives. They are simple, rugged, inexpensive, and available at all power ratings. Progress in the field of power electronics and microelectronics enables the application of induction motors for high-performance drives, where traditionally only DC motors were applied. Thanks to sophisticated control methods, AC induction drives offer the same control capabilities as high-performance four-quadrant DC drives.

ACIM is an excellent choice for appliance and industrial applications. This design will employ sensorless Field-Oriented Control (FOC) to control an ACIM using the 56F8013 device, which can accommodate the sensorless FOC algorithm. A motor control system is flexible enough to implement a washing machine protocol while it drives a variable load. The system illustrates the features of the 56F8013 in motor control. The flexible Human Machine Interface (HMI) allows the control board to communicate with a PC and supports a simplified HMI using push buttons on the processor board, making the system easy to use.

This document describes the Freescale 56F8013 controller’s features, basic AC induction motor theory, the system design concept, and hardware implementation and software design, including the PC master software visualization tool.

Chapter 2
Benefits and Features of the 56F8013 Controller

2.1 56F8013 Benefits

- Hybrid architecture facilitates implementation of both control and signal processing functions in a single device
- High-performance, secured Flash memory eliminates the need for external storage devices
- Extended temperature range allows for operation of nonvolatile memory in harsh environments
- Flash memory emulation of EEPROM eliminates the need for external non-volatile memory
- High performance with 16-bit code density
- On-chip voltage regulator and power management reduces overall system cost
- Diversity of peripheral configuration facilitates the elimination of external components, improving system integration and reliability
- This device boots directly from Flash, providing additional application flexibility
- High-performance Pulse Width Modulation (PWM) with programmable fault capability simplifies design and promotes compliance with safety regulations
- PWM and Analog-to-Digital (ADC) modules are tightly coupled, reducing processing overhead
- Low-voltage interrupts protect the system from brownout or power failure
- Simple in-application Flash memory programming via Enhanced OnCE™ or serial communication

2.2 56800E Core Features

- Up to 32 MIPS at 32MHz execution frequency
- DSP and MCU functionality in a unified, C-efficient architecture
- JTAG/Enhanced On-Chip Emulation (EOnCE) for unobtrusive, real-time debugging
- Four 36-bit accumulators
- 16- and 32-bit bidirectional barrel shifter
- Parallel instruction set with unique addressing modes
- Hardware DO and REP loops available
- Three internal address buses
- Four internal data buses
- Architectural support for 8-, 16-, and 32-bit single-cycle data fetches
- MCU-style software stack support
- Controller-style addressing modes and instructions
- Single-cycle 16 x 16-bit parallel Multiplier-Accumulator (MAC)
- Proven to deliver more control functionality with a smaller memory footprint than competing architectures

2.3 Memory Features

- Architecture permits as many as three simultaneous accesses to program and data memory
- On-chip memory includes high-speed volatile and nonvolatile components:
  - 16KB of Program Flash
  - 4KB of Unified Data/Program RAM
- All memories operate at 32MHz (zero wait-states) over temperature range (-40° to +125°C), with no software tricks or hardware accelerators required
- Flash security feature prevents unauthorized accesses to its content

2.4 56F8013 Peripheral Circuit Reatures

- Pulse Width Modulator (PWM) module
- Serial Peripheral Interface (SPI)
- Serial Communication Interface (SCI)
- Four 16-bit Timers
- Software-programmable Phase Lock Loop (PLL)
- Two 12-bit Analog-to-Digital Converters (ADC) with six inputs at rates up to 1.1µs per sequential or simultaneous conversion
- Up to 26 General Purpose I/O (GPIO) pins
- Computer Operating Properly (COP)
- Integrated Power-On Reset and Low-Voltage Interrupt module
- I^2C Communication Module supporting Slave, Master and MultiMaster Mode

2.5 AWARD-WINNING DEVELOPMENT ENVIRONMENT

Processor Expert (PE) provides a Rapid Application Design (RAD) tool that combines creation of an easy-to-use, component-based software application with an expert knowledge system.

The CodeWarrior Integrated Development Environment (IDE) is a sophisticated tool for code navigation, compiling, and debugging. A complete set of evaluation modules (EVMs) and development system cards will support concurrent engineering. Together, PE, CodeWarrior, and EVMs create a complete, scalable tools solution for easy, fast, and efficient development.

Chapter 3
Motor Drive System

3.1 Introduction

An AC Induction Motor (ACIM), which is simple, rugged, inexpensive, and available at all power ratings, is often used in products targeting the consumer and industrial market. This application employs sensorless Field-Oriented Control (FOC) to control an ACIM using the 56F8013 device, which can support the complicated sensorless FOC algorithm. By using this algorithm, the motor drive system achieves excellent torque control performance and supports the driving of variable loads.

3.2 Features of a Motor Drive System

- The design implements the washing machine protocol, shown in **Figure 3-1**

Figure 3-1. Washing Machine Protocol

- The design also fulfills the requirements of the washing cycle, shown in **Figure 3-2**

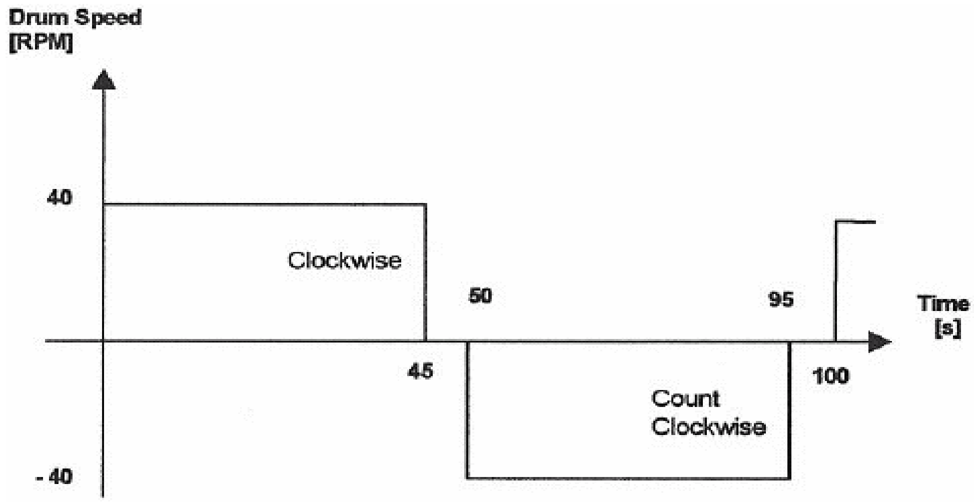

Figure 3-2. Washing Cycle

- The motor control algorithm employs Stator-Flux-Oriented Control (SFOC); Power stage switches are controlled by Space Vector Pulse Width Modulation (SVPWM)
- No position information devices or stator flux measurement are used, so a speed sensorless method is employed
- The motor is capable of forward and reverse rotation and has a speed range from 50rpm to 3000rpm; the tumble wash has a speed of 40rpm and the spin cycle obtains a maximum drum speed of 1600rpm. The drum can be driven directly or by a belt that connects to the motor shaft. To acheive the wash and spin cycles, the speed-transfer ratio can be set at 1:2.
- The user controls motion profiles, rotation direction, and speed. The RS-232 communication supports further R&D by enabling the easy tuning of control parameters.
- The motor drive system is designed to create minimal acoustic noise

3.3 Introduction to System Design

3.3.1 Hardware

This application uses a 56F8013 device to drive a 3-phase motor with a complicated motion protocol. The resistor uses phase current sensors and no optocoupler, so the system is cost-sensitive.

PC master software communicates with the PC through the RS-232 and senses the mid-variables and modifies the control-variables during the debug process.

The system comprises a 56F8013 board and an ACIM board. The ACIM board includes a 3-phase power stage, Power Factor Correction (PFC), a communication module which links the PC with the 56F8013 demonstration, simplified Human Machine Interface (HMI) and a protection module, as well as effective electrical isolation.

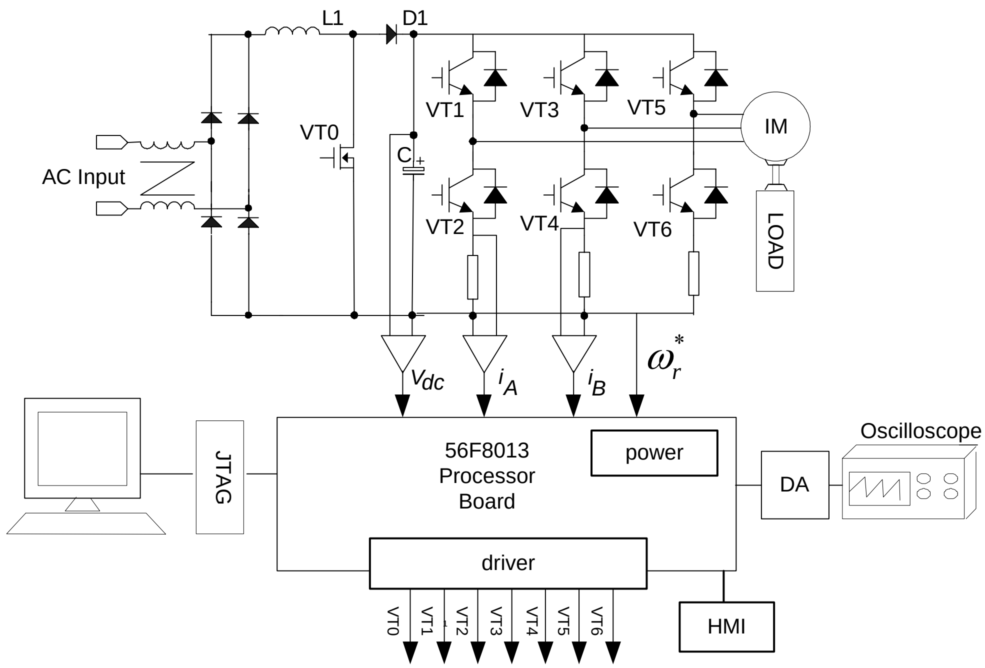

Figure 3-3. System Block Diagram

Among the hardware system features are:

- **Integrated Power Module (IPM)**
  An IRAMS10UP60A, a 600V, 10-Ampere IR Integrated Power Module, powers the ACIM. Its built-in control circuits provide optimum gate drive and protection for the IGBT. Three bridges are integrated in its body. It reduces the design scale of hardware and software. Figure 3-4 shows the Circuit Diagram.

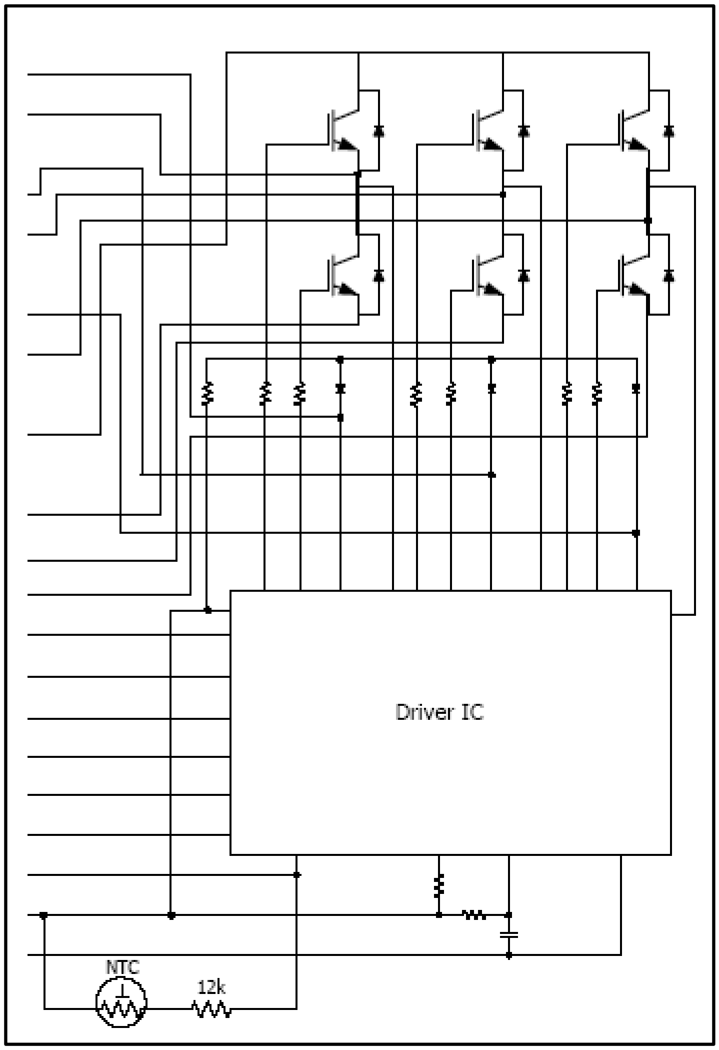

Figure 3-4. IRAMS10UP60A Circuit Diagram

- **56F8013**
  Guaranteeing excellent performance and accurate control of the ACIM requires more complex software, but the powerful 56F8013 is capable of the heavy computation demanded.

  The controller board includes:
  — Control system circuit
  — CPU circuit
  — ADC circuit
  — Power supply circuit
  — DAC circuit
  — SCI interface
  — Parallel JTAG interface
  — LED display circuit
  — Signals output interface

- **No optocoupler**
  To keep the application's costs low, optocouplers are not used as an interface between the controller and the IPM. A reliable protection circuit improves system safety.
- **Power stage for ACIM, BLDC, and PMSM**
  The power stage can drive ACIM, BLDC, and PMSM motors with only minor adjustments to resistor values
- **Signal sample and process board**
  To control hardware costs, rather than using a Hall effect transducer, a simple difference amplier circuit detects the current and voltage signals
- **56F8013 Evaluation Module (EVM)**
  Freescale's 56F8013 demostration board connects to the main board and highlights the capability of the EVM

3.3.2 Software

This system drives a 3-phase ACIM using stator-flux orientation. The application features:

- Control technique, which includes:
  — Phase currents and phase voltages reconstruction
  — Stator-flux observation
  — Electromagnetic torque estimation, used for the slip frequency calculation
  — Stator flux orientation to calculate the torque-producing stator current to be used in the speed regulation channel
  — Speed closed loop, allowing the motor a good transient response
  — Compensation for the voltage drops across the stator resistor
  — SVPWM to generate the desired voltage by the inverter
- Minimum speed of 50rpm
- Maximum speed of 3000rpm
- Power factor correction which eliminates negative effects on the input electric use of switches
- Fault protection against:
  — Bus overvoltage
  — Bus undervoltage
  — Bus overcurrent
  — IPM overheating
- PC master software for debug and remote control of the ACIM

3.4 Specification and Performance

Input voltage:	85~265VAC
Input frequency:	45~65HZ
Rating bus voltage:	350V
Rating output power:	500W
Switch frequency of PFC switch:	100KHZ
Switch frequency of inverter:	10KHZ
Power factor:	>95%
Efficiency:	>90%

Chapter 4
ACIM Theory

4.1 AC Induction Motor

Squirrel-cage AC induction motors are popular for their simple construction, low cost per horsepower, and low maintenance (they contain no brushes, as do DC motors). They are available in a wide range of power ratings. With field-oriented vector control methods, AC induction motors can fully replace standard DC motors, even in high-performance applications. The AC induction motor is a rotating electric machine designed to operate from a 3-phase source of alternating voltage. In variable-speed drives, the source is normally an inverter that uses power switches to produce approximately sinusoidal voltages and currents of controllable magnitude and frequency.

As the sinusoidally-distributed flux density wave produced by the stator magnetizing currents sweeps past the rotor conductors, it generates a voltage in them. The result is a sinusoidally distributed set of currents in the short-circuited rotor bars. Because of the low resistance of these shorted bars, only a small relative angular velocity, ω_r, between the angular velocity, ω_s, of the flux wave and the mechanical angular velocity, ω, of the two-pole rotor is required to produce the necessary rotor current. The relative angular velocity, ω_r, is called the slip velocity. The interaction of the sinusoidally distributed air gap flux density and induced rotor currents produces a torque on the rotor. The typical induction motor speed-torque characteristic is shown in **Figure 4-1**.

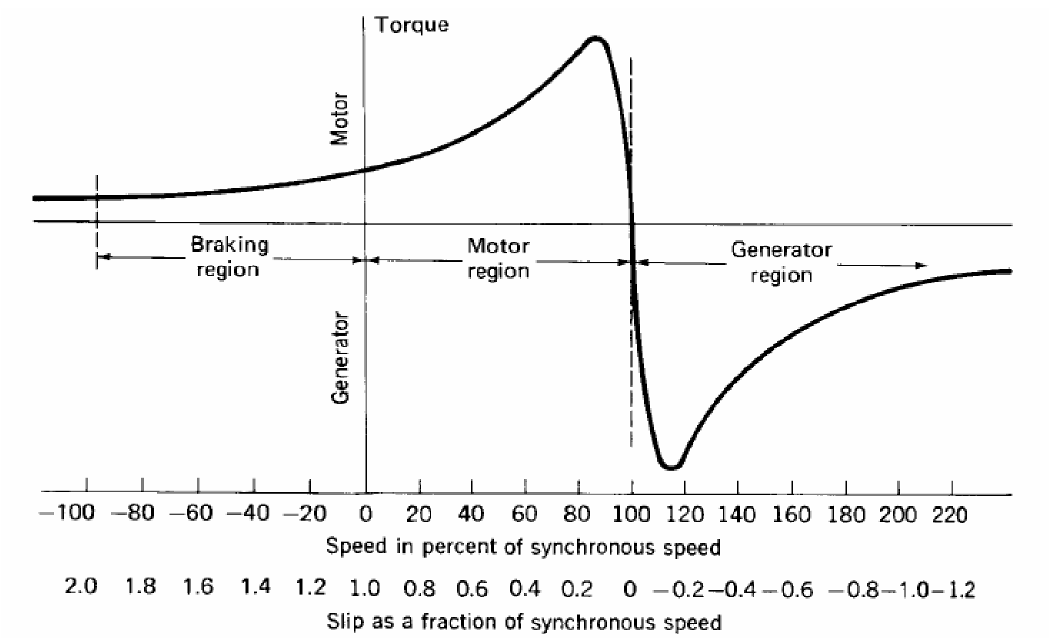

Figure 4-1. Induction Motor Speed-Torque Characteristic

4.2 Induction Motor Model

Stator voltage differential equation:

$$\vec{U}_s = R_s\vec{i}_s + p\vec{\Psi}_s + j\omega_1\vec{\Psi}_s$$

Eqn. 4-1

Rotor voltage differential equation:

$$0 = R_r\vec{i}_r + p\vec{\Psi}_r + j\omega_s\vec{\Psi}_r$$

Eqn. 4-2

Stator and rotor flux linkages expressed in terms of the stator and rotor current space vectors:

$$\vec{\Psi}_s = L_s\vec{i}_s + L_m\vec{i}_r$$

Eqn. 4-3

$$\vec{\Psi}_r = L_r\vec{i}_r + L_m\vec{i}_s$$

Eqn. 4-4

Electromagnetic torque expressed by utilizing space vector quantities:

$$T_e = n_p(\vec{\Psi}_s \times \vec{i}_s)$$

Eqn. 4-5

Where:

$\vec{U}_s$	Stator voltage vector
$\vec{\Psi}_s$	Stator flux vector
$\vec{\Psi}_r$	Rotor flux vector
$\vec{i}_s$	Stator current vector
$\vec{i}_r$	Rotor current vector
L_s	Stator equivalent inductance
L_r	Rotor equivalent inductance
L_m	Mutual equivalent inductance
n_p	Pole pairs
T_e	Electormagnetic torque
ω_1	Synchronous speed frequency
ω_s	Synchronous slip frequency

4.3 Digital Control of an AC Induction Motor

In adjustable-speed applications, AC motors are powered by inverters, which convert DC power to AC power at the required frequency and amplitude. Figure 4-2 shows the hardware system configuration.

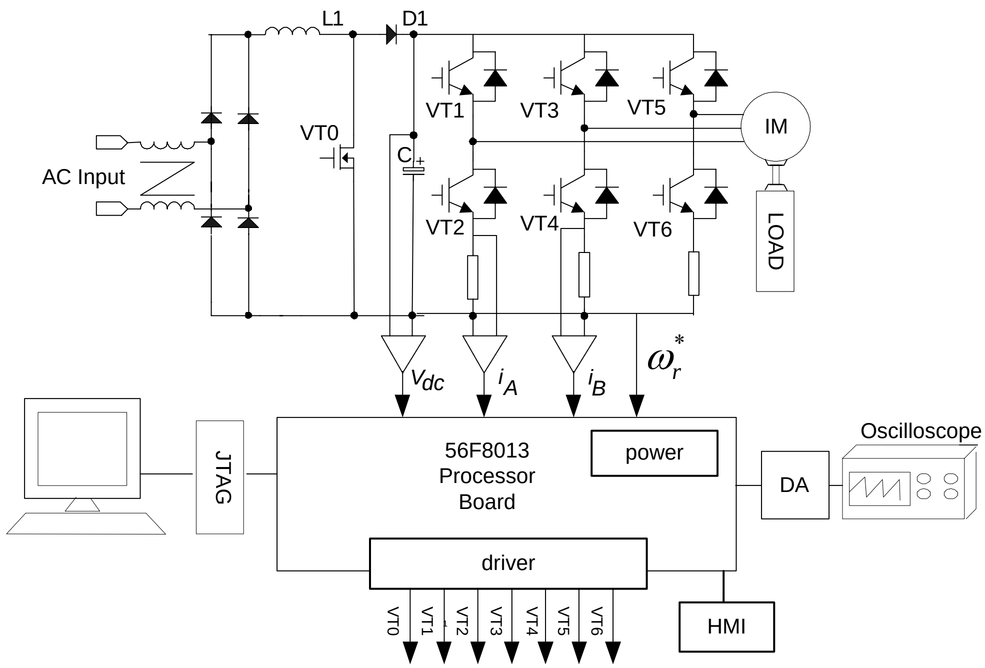

Figure 4-2. Hardware System Configuration

The inverter consists of three half-bridge units in which the upper and lower switch are controlled complementarily, meaning when the upper one is turned on, the lower one must be turned off, and vice versa. Some dead time must be inserted between the time one transistor of the half-bridge is turned off and its complementary device is turned on.

The output voltage is mostly created by a Pulse Width Modulation (PWM) technique, where an isosceles triangle carrier wave is compared with a fundamental-frequency sine modulating wave. This technique is shown in Figure 4-3. The 3-phase voltage waves are shifted 120° to one another and thus a 3-phase motor can be supplied.

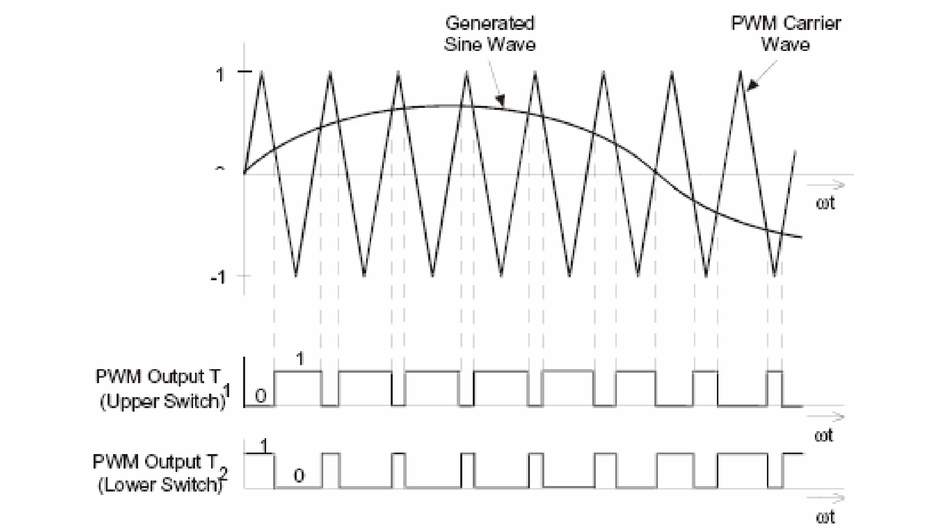

Figure 4-3. Pulse Width Modulation

In this document, the Space Vector Pulse Width Modulation (SVPWM) is employed to reduce the harmonic distortion and improves the efficient use of the bus voltage. Two basic neighboring voltage vectors are used to compose the arbitary voltage vector in the control period.

The most popular power devices for motor control applications are Power MOSFETs and IGBTs. A Power MOSFET is a voltage-controlled transistor. It is designed for high-frequency operation and has a low-voltage drop, so it has low power losses. An Insulated-Gate Bipolar Transistor (IGBT) is controlled by a MOSFET on its base. A built-in temperature monitor and overtemperature/overcurrent protection, along with the short-circuit rated IGBTs and integrated under-voltage lockout function, make the Integrated Power Module (IPM) more convenient for engineers to develop their systems and make IPMs widely used in today’s home appliances. This application also incorporates an IPM.

Chapter 5
Design Concept of an ACIM Vector Control Drive

5.1 Vector Control of AC Induction Machine

Aligning the d axis to the stator flux, $\vec{\Psi}_s$, written in d-q component, stator voltage is then transformed to:

$$u_{ds} = R_s i_{ds} + p\Psi_s \quad \text{Eqn. 5-1}$$

$$u_{qs} = R_s i_{qs} + \Psi_s \omega_1 \quad \text{Eqn. 5-2}$$

From **Equation 4-2** to **Equation 4-4**, the following equations can be derived:

$$(1+\sigma\tau_r p)L_s i_{sq} - \omega_s \tau_r (\Psi_s - \sigma L_s i_{sd}) = 0 \quad \text{Eqn. 5-3}$$

$$(1+\tau_r p)\Psi_s = (1+\sigma\tau_r p)L_s i_{sd} - \omega_s \sigma \tau_r L_s i_{sq} \quad \text{Eqn. 5-4}$$

then:

$$T_e = n_p i_{sq} \Psi_s \quad \text{Eqn. 5-5}$$

where:

τ_r	Rotor Time Constant
$\sigma = 1 - \frac{L_m^2}{L_s L_r}$	Total Leakage Factor

Equation 5-4 indicates the coupling between i_{sd} and i_{sq}. **"A Stator Flux Oriented Induction Machine Drive"** presents a method to decouple the i_{sd} from i_{sq} using a decouple compensator. However, the use of a decouple compensator will negatively affect the system performance, depending on the machine parameters, and increase software complexity. **Equation 5-1** represents the relationship between stator flux, Ψ_S, and the d-axis stator voltage. The differential will introduce noise, so a Proportional-Integral (PI) flux regulator is used to approach the effect of stator voltage on flux, as shown in **Equation 5-6**:

$$u_{ds} = K_p(\Psi_s^* - \hat{\Psi}_s) + K_i \int (\Psi_s^* - \hat{\Psi}_s)dt \quad \text{Eqn. 5-6}$$

where:

Ψ^*_S	Commanded Stator Flux
$\hat{\Psi}^*_S$	Estimated Stator Flux

This information allows calculation of voltage on the d axis.

Assuming $R_s i_{qs} << \Psi_s \omega_1$, **Equation 5-2** will simplified to:

$$u_{qs} \approx \Psi_s \omega_1$$

Eqn. 5-7

In the steady state, u_{qs} is proportional to ω_1 and, in a sense, ω_1 possesses a characteristic of the constant volts/hertz ratio, but at the low speed range, $R_s i_{qs}$ can't be ignored.

From **Equation 5-2** and **Equation 5-6**, the terminal reference voltage vector, $\vec{V}_{ref}$ can be established as shown in **Figure 5-1**, where ω^*_1 is the commanded synchronous speed.

$$\theta = \int \omega_1^* dt = \omega_1^* T_c + \theta_0$$

Eqn. 5-8

From **Figure 5-1**, it is clear that u_{qs} takes up the majority of $\vec{V}_{ref}$, while u_{ds} compensates the stator flux loss due to the voltage drop across the stator resistance in the transient state.

Based on the analysis, the control scheme can be obtained as shown in **Figure 5-2**.

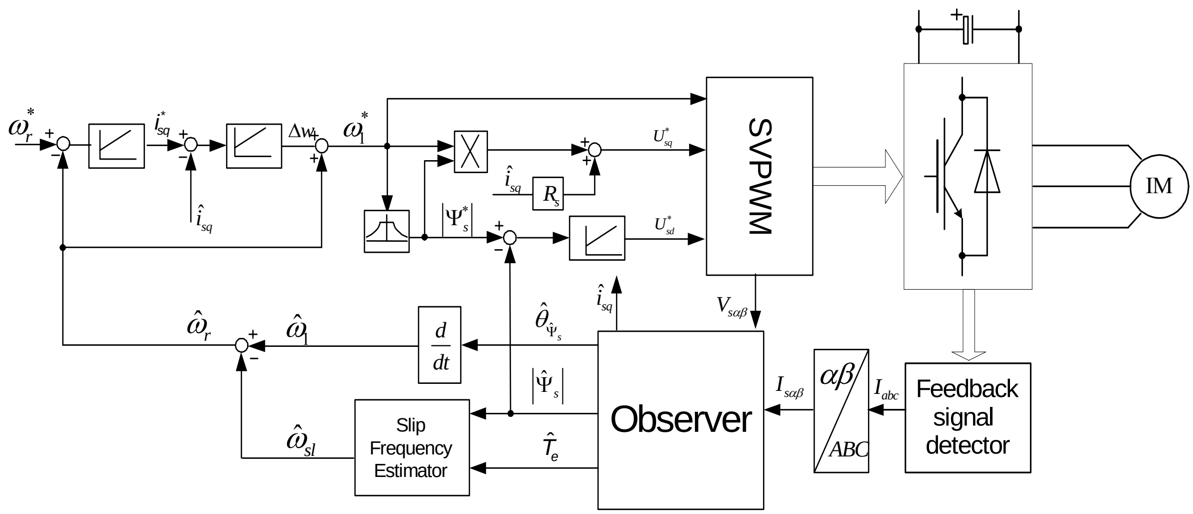

Figure 5-1. Block Diagram of the Stator Flux Oriented (SFO) System

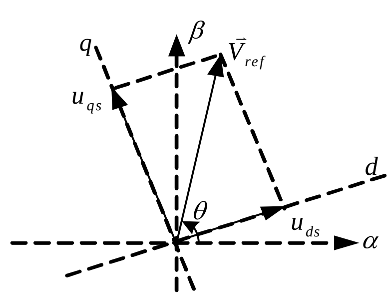

Figure 5-2. Stator Reference Voltage $\vec{V}_{ref}$

5.2 Relationship between Rotor Flux Orientation and Stator Flux Orientation Induction Motor Drive

The aim of vector control is to implement control schemes which produce high-dynamic performance and are similar to those used to control DC machines. To achieve this, the reference frames may be aligned with the stator flux-linkage space vector, the rotor flux-linkage space vector, or the magnetizing space vector.

From **Equation 4-3** and **Equation 4-4**, the relationship between stator flux and rotor flux can be calculated as follows:

$$\vec{\Psi}_s = \int (\vec{U}_s - r_s \vec{i}_s) dt$$

Eqn. 5-9

$$\vec{\Psi}_r = \frac{L_r}{L_m} (\vec{\Psi}_s - \sigma L_s \vec{i}_s)$$

Eqn. 5-10

Equation 5-9 indicates that the stator flux depends only on the stator resistance, which is relatively easy to calculate. **Equation 5-10** demonstrates that the rotor flux requires the knowledge of instances of the machine, especially the leakage inductance. The rotor flux estimation suffers when machine parameters are detuned. When the estimated value of a parameter differs from its actual value, the estimated rotor flux is then different from the actual rotor flux. The orientation is no longer accurate with respect to the actual rotor flux. In this case, the system becomes coupled, and instantaneous torque control is lost.

The stator flux can be estimated more easily and precisely than the rotor flux. Thus, the Stator Flux Oriented (SFO) system has been attracting more attention. However, a coupling exists between the torque-producing component of the stator current i_{sq} and the stator flux-producing component. Consequently, any change in i_{sq} without a corresponding change in i_{sd} will cause a transient in stator flux. See **"A Stator Flux Oriented Induction Machine Drive"**. Accurate decoupling control still depends on knowledge of machine parameters.

This application illustrates an ACIM drive using stator flux orientation, without the use of a speed sensor.

5.3 Block diagram of Stator Flux Oriented (SFO) Control

Figure 5-2 shows the basic structure of SFO control of an AC induction motor. To perform vector control, follow these steps:

1. Measure bus voltage and phase currents
2. Transform these measurements into a 2-phase system using Clarke transformation
3. Estimate stator flux and slip frequency
4. Calculate synchrounous speed, then rotor speed
5. Calculate the torque-producing current, i_{sq}
6. Use the PI regulator to obtain the commanded slip frequency
7. Add the commanded slip frequency to the estimated rotor speed to find the commanded synchronous speed
8. Use the compensation method to obtain the stator voltage on the direct axis and quadrature axis.
9. Use SVPWM to generate stator voltage

5.4 Forward and Inverse Clarke Transformation (a, b, c to □α , β and backwards)

The forward Clarke transformation converts a 3-phase system (a, b, c) to a 2-phase coordinate system (α, β). **Figure 5-3** shows graphical construction of the space vector and projection of the space vector to the quadrature-phase components, α, β. Assuming that the a axis and the α axis are in the same direction, the quadrature-phase stator currents $i_{s\alpha}$ and $i_{s\beta}$ are related to the actual 3-phase stator currents as follows:

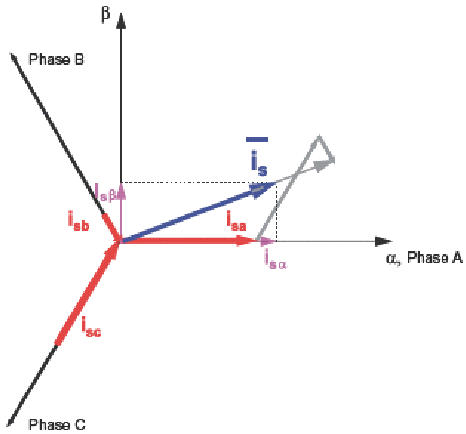

Figure 5-3. Clark Transformation

$$i_{s\alpha} = i_{sa} \qquad \textit{Eqn. 5-11}$$

$$i_{s\beta} = \frac{1}{\sqrt{3}} i_{sa} + \frac{2}{\sqrt{3}} i_{sb} \qquad \textit{Eqn. 5-12}$$

The inverse Clarke transformation transforms from a 2-phase (α, β) to a 3-phase (i_{sa}, i_{sb}, i_{sc}) system.

$$i_{sa} = i_{s\alpha} \qquad \textit{Eqn. 5-13}$$

$$i_{sb} = -\frac{1}{2} i_{s\alpha} + \frac{\sqrt{3}}{2} i_{s\beta} \qquad \textit{Eqn. 5-14}$$

$$i_{sb} = -\frac{1}{2} i_{s\alpha} + \frac{\sqrt{3}}{2} i_{s\beta} \qquad \textit{Eqn. 5-15}$$

5.5 Forward and Inverse Park Transformation (α, β to d-q and backwards)

In stator-vector oriented control, the quanties in the statar reference frame should be transformed into the synchronous rotation with the stator flux vector reference frame. The relationship of the two reference frames is shown in Figure 5-4. The d axis is aligned with the stator flux vector, where $\theta_{\bar{\Psi} s}$ is the position of the stator flux.

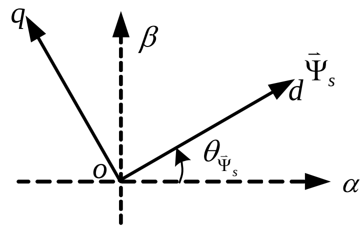

Figure 5-4. Park Tranformation

The quantity in the stationary frame is transformed into synchrounous frame by:

$$i_{sd} = i_{s\alpha}\cos\theta_{\bar{\Psi}_s} + i_{s\beta}\sin\theta_{\bar{\Psi}_s}$$ ***Eqn. 5-16***

$$i_{sq} = -i_{s\alpha}\sin\theta_{\bar{\Psi}_s} + i_{s\beta}\cos\theta_{\bar{\Psi}_s}$$ ***Eqn. 5-17***

And the inverse relation is:

$$i_{s\alpha} = i_{sd}\cos\theta_{\bar{\Psi}_s} - i_{sq}\sin\theta_{\bar{\Psi}_s}$$ ***Eqn. 5-18***

$$i_{s\beta} = i_{sd}\sin\theta_{\bar{\Psi}_s} + i_{sq}\cos\theta_{\bar{\Psi}_s}$$ ***Eqn. 5-19***

5.6 Rotor Speed Estimation

The synchronous frequency can be calculated:

$$\hat{\omega}_1 = \frac{d}{dt}(\hat{\theta}_{\hat{\Psi}_s}) = \frac{d}{dt}\arctan(\frac{\hat{\Psi}_{s\beta}}{\hat{\Psi}_{s\alpha}}) = \frac{(u_{s\beta} - R_s i_{s\beta})\hat{\Psi}_{s\alpha} - (u_{s\alpha} - R_s i_{s\alpha})\hat{\Psi}_{s\beta}}{\hat{\Psi}_s^2}$$ ***Eqn. 5-20***

where:

$u_{s\alpha}$, $u_{s\beta}$, $i_{s\alpha}$, $i_{s\beta}$ are the stator voltage and current in the α—β stationary reference frame.

Slip frequency can be deduced from Equation 5-3:

$$\hat{\omega}_s = \frac{(1 + \sigma\tau_r p)L_s\hat{i}_{sq}}{\tau_r(\hat{\Psi}_s - \sigma L_s\hat{i}_{sd})}$$ ***Eqn. 5-21***

It will add to the software complexity to calculate $\hat{\omega}_S$ using **Equation 5-21**, and the detuning of the parameters will affect the rotor speed calculation.

Slip frequency can be derived from nameplate specification of the induction machine, as shown in **Table 5-1**.

Table 5-1. Nameplate Specification

Rated Power	0.12kw	Rated Speed	1310rpm
Rated Current	0.76A	Rated Frequency	50Hz
Rated Voltage	220V	Pole Pairs	2

Slip frequency is obtained by:

$$\Delta\omega_N = \frac{(1500\text{-}1310)\text{rounds}}{\text{minute}} = \frac{(1500\text{-}1310)\text{r} \times p_n}{60\text{seconds}} = 6.3Hz$$

Eqn. 5-22

Estimated slip frequency can be determined by the observer of electric torque:

$$slip\_estimated = \frac{\Delta\omega_N}{T_{eN}} \times \hat{T}_e = \frac{6.3Hz}{0.875} \times \hat{T}_e = 7.2 \times \hat{T}_e$$

Eqn. 5-23

Therefore, the rotor speed can be calculated:

$$\hat{\omega}_r = \hat{\omega}_1 - \hat{\omega}_s$$

Eqn. 5-24

5.7 Speed Regulator

From **Equation 5-5**, the torque is in proportion to the torque-producing current i_{sq} . Quick control on i_{sq} will yield a fast transient state. The PI speed regulator generates the command i^*_{sq} from the difference between the commanded rotor speed and estimated rotor speed. Commanded slip frequency can then be obtained by the difference between the commanded i_{sq} and estimated $\hat{i}_{sq}$ through another PI regulator. The reference synchronous speed is calculated by finding the sum of the estimated rotor speed and commanded slip frequency.

The speed regulator channel can be found as shown in **Figure 5-5**.

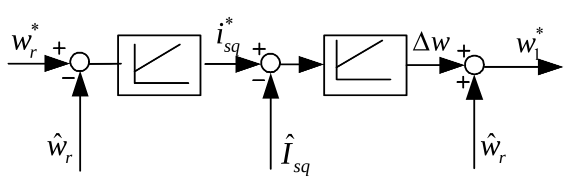

Figure 5-5. Speed Regulator Channel

5.8 PFC Design

The main circuit adopted in this application is a single-switch PFC circuit (see Figure 5-6). The circuit is composed of Q, D, L, and filter capacitance, C2, C3 and includes an EMI filter, input relay, and full-wave rectifier. In the 56F8013-based PFC module system, the controller samples the voltage signal output and voltage *DC_bus*, and processes these samples in the digital control loop. Because system is based on current Discontinuous Current Mode (DCM) mode, there is only a voltage loop. Outer voltage loop G insures the output voltage is constant.

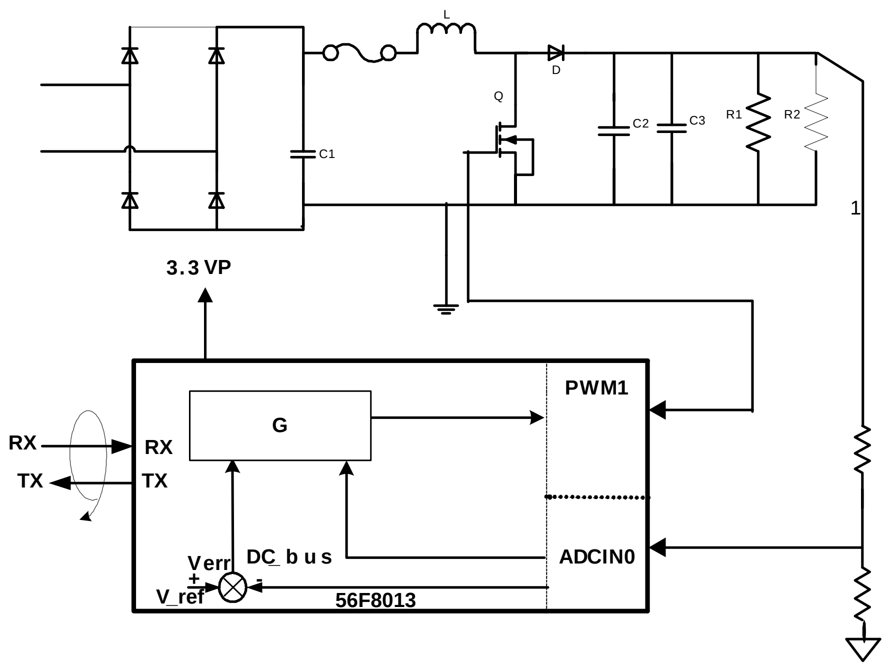

Figure 5-6. PFC Configuration Diagram

5.8.1 Inductor selection

A. Maximum peak line current:

$$I_{pk(\max)} = \frac{\sqrt{2} \times P_O}{\eta V_{in(\min)}} = \frac{\sqrt{2} \times 500}{0.9 \times 85} = 9.24A$$

Eqn. 5-25

Ripple current:

$$\Delta I_L = 20\% I_{pk} = 0.2 \times 9.24 = 3.7A$$

Eqn. 5-26

B. Determine the duty factor at I_{pk}, where $V_{in(peak)}$ is the peak of the rectified line voltage.

$$D = \frac{V_o - V_{in(peak)}}{V_o} = \frac{380 - \sqrt{2} \times 85}{380} = 0.68$$

Eqn. 5-27

C. Calculate the inductance; f_S is the switching frequency.

$$L = \frac{V_{in} \times D}{fs \times \Delta I} = \frac{\sqrt{2} \times 85 \times 0.68}{100000 \times 3.7} = 221\ \mu H$$

Eqn. 5-28

Round up to 250µH.

5.8.2 Output Capacitor

Output filter inductor can be calculated by the following equation:

$$C = \frac{2 \times P_O \times \Delta t}{V_{O(max)}^2 - V_{O(min)}^2}$$

Eqn. 5-29

$P_o = 500W$
$V_{o(min)} = 380 \text{ x } (1 - 10\%) = 342V$
$V_{o(max)} = 380 \text{ x } (1+10\%) = 418V$
$\Delta t = 50\text{ms}$

According to **Equation 5-29**, C = 866µH.
Select the output capacitor to be C = 940µH.
Two 470µH/450*V* electrolytic capacitors connected in parallel are chosen.

5.8.3 Main Switch

The voltage limit of the main switch is:

$$V_{CEM(S)} > 1.5V_{cem(S)} = 1.5V_{in(max)} = 1.5 \text{ x } 380 = 570V$$ ***Eqn. 5-30***

The circuit limit of the main switch is calculated by RMS value:

$$I_{CEM(S)} > 1.5 I_{L(max)} = 1.5 \times \frac{\sqrt{2} \cdot P_O}{\eta \cdot V_{in(min)}} = 1.5 \times \frac{\sqrt{2} \cdot 500}{0.9 \times 85} = 13.86\ A$$

Eqn. 5-31

Select main switch Q_{400}—Q_{401} to be the MOSFET IRFPC60LC. Parameters are described as follows:
$V_{DSS} = 600V$
$I_D = 16A$
R_{DS} *(on) tye* = 0.4Ω
TO-247AC Package

5.8.4 Output Diode

The voltage limit of the output diode is:

$$V_{CEM(S)} > 1.5V_{cem(S)} = 1.5V_{in(max)} = 1.5 \text{ x } 380 = 570V$$ ***Eqn. 5-32***

The circuit limit of the output diode is calculated by RMS value:

$$I_{CEM(S)} > 1.5 I_{L(max)} = 1.5 \times \frac{\sqrt{2} \cdot P_O}{\eta \cdot V_{in(min)}} = 1.5 \times \frac{\sqrt{2} \cdot 500}{0.9 \times 85} = 13.86\ A$$

Eqn. 5-33

Select output diode D_{400}—D_{402} to be FRED DSEP60-06A. Parameters are described as follows:
$V_{RRM} = 600V$
$I_{FAVM} = 60A$
$t_{rr} = 35nS$
TO-247AD Package

5.8.5 Inductor Design

In **Section 5.8.1**, it was found that L= 250µH.
Select Bm= 0.3T.
Select magnetic core to be EI33, with an effective area of 118mm^2.

The number of inductor windings can be calculated as follows:

$$N = \frac{LI_{L(\max)}}{A_e B_m} = 38.2$$

Eqn. 5-34

Select N = 38.The gap is:

$$\delta = \frac{\mu_o N^2 A_e}{L} = \frac{1.25\times10^{-6}\times38^2\times118\times10^{-6}}{250\times10^{-6}} = 0.85mm$$

Eqn. 5-35

When work frequency of inductance is 100kHz, the penetrate depth of copper lead is:

$$\Lambda = \sqrt{\frac{2}{2\pi f_s \mu\gamma}} = \sqrt{\frac{1}{3.14\times100\times10^3\times1.25\times10^{-6}\times58\times10^6}} = 0.209mm$$

Eqn. 5-36

Where:
γ is the electric conductive ratio of lead
µ is magnetical conductive ratio of lead

A copper lead with a smaller diameter than 0.42mm can be selected. In this case, select high intensity lead with a diameter of 0.33mm and an effective area of 0.0855mm^2.

By selecting circuit density to be J = 3.5A/mm^2,the area of leads is $S = \frac{3.84}{3.5} = 1.1\text{mm}^2$.
Thirteen leads with a diameter of 0.33mm must be used.

$$Kc = \frac{38\times13\times0.0855}{132} = 0.32 \ll 0.35$$

Eqn. 5-37

Chapter 6
Hardware Implementation

The motor control system is designed to drive the 3-phase AC motor in a speed closed loop. The prototype is pictured in **Figure 6-1** and It consists of the following blocks:

- 56F8013
- High-voltage power stage board with sensor board
- Power supply stage and PFC
- 3-Phase AC motor without speed transducer

6.1 56F8013 Device

The demonstration system is illustrated in **Figure 6-1** and the hierarchy diagram is depicted in **Figure 6-2**. it clearly shows that the 56F8013 is the core of the system, highlighted atop the mother board. **Figure 6-3** shows the motor control system configuration.

Figure 6-1. Demonstration System

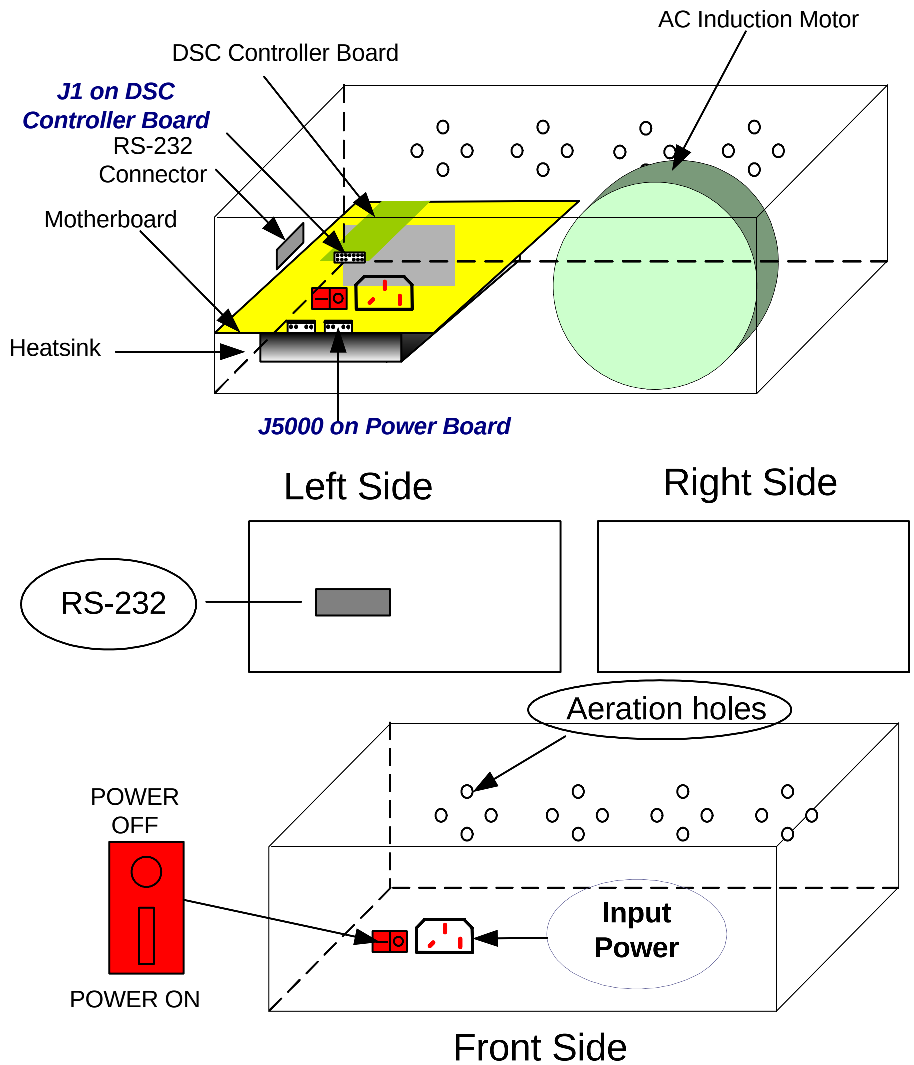

Figure 6-2. Hierarchy Diagram

The 56F8013 is the drive's brain. All algorithms are carried out in this single smart chip, which reads the input commands, processes the routine, and generates the PWM to govern the power switches driving the motor and the PFC to make the input current sinusoid.

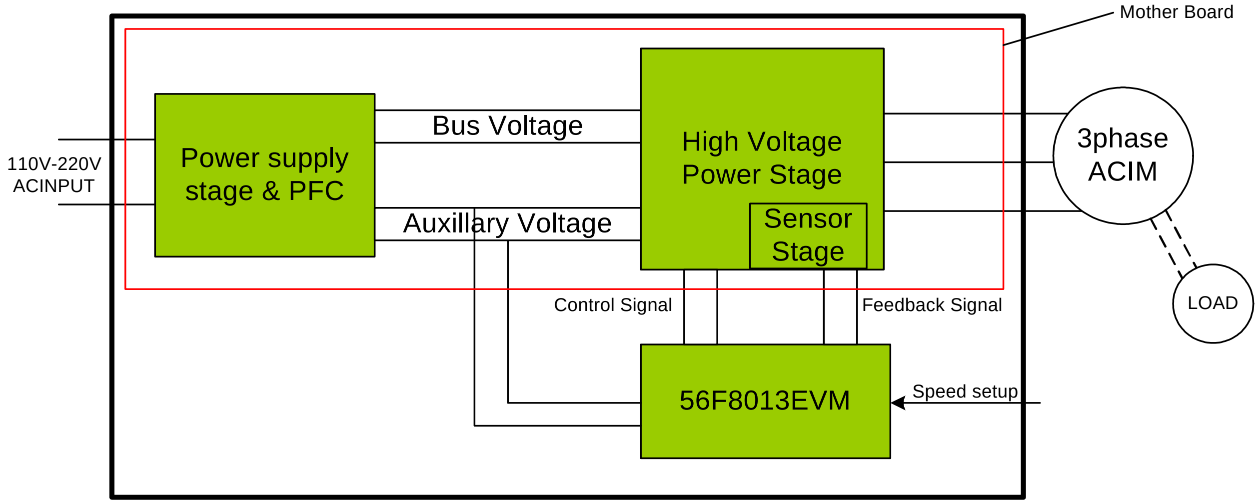

Figure 6-3. Motor Control System Configuration

6.2 High-Voltage Power Stage

The HV Medium Power Board is designed to meet the power needed by a household washing machine and lower-power industrial applications. An Integrated Power Module (IPM) is used to simplify the design and board layout and to lower the cost. IPMs are available from various suppliers and it is simple to use one from a supplier of choice. The IRAMS10UP60A is an IPM, which targets the household appliance market. Its features include:

- Integrated gate drivers and bootstrap diodes
- Temperature monitor
- Temperature and overcurrent shutdown
- Fully isolated package
- Low VCE (on) non-punch-through IGBT technology
- Undervoltage lockout for all channels
- Matched propagation delay for all channels
- Low-side IGBT emitter pins for current conrol
- Schmitt-triggered input logic
- Cross-conduction prevention logic
- Lower di/dt gate driver for better noise immunity

Its maxium IGBT block voltage is 600V; phase current is 10A at 25°C and 5A at 100°C, making it suitable for this appliance.

6.3 Sensor Stage

The control algorithm requires DCBus voltage, DCBus current and phase current sensing, so these sensors are built on the power stage board. Schematics of the sensors circuits can be found in **Appendix A**.

A. DCBus Voltage Sensor

The DCBus voltage must be checked because overvoltage protection and PFC are required. A simple voltage sensor is created by a diffential amplifier circuit. The voltage signal is transferred through a resistor and then amplified to the reference level. The amplifier output is connected to the 56F8013's ADC.

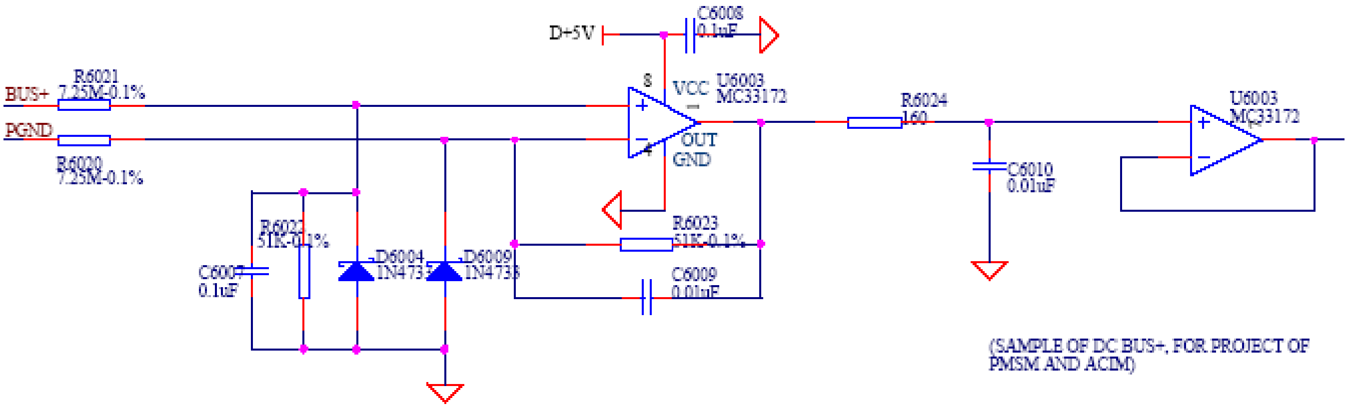

Figure 6-4. DCBus Sampling Circuit

B. DCBus Current Sensor

The bus current is sensed through the detection of the voltage drop across the resistor cascade into the negative bus link. A differential amplifier is then used to draw the voltage out and transform it to a level the 56F8013's AD channel can accommodate. The sample circuit is depicted in **Figure 6-5**.

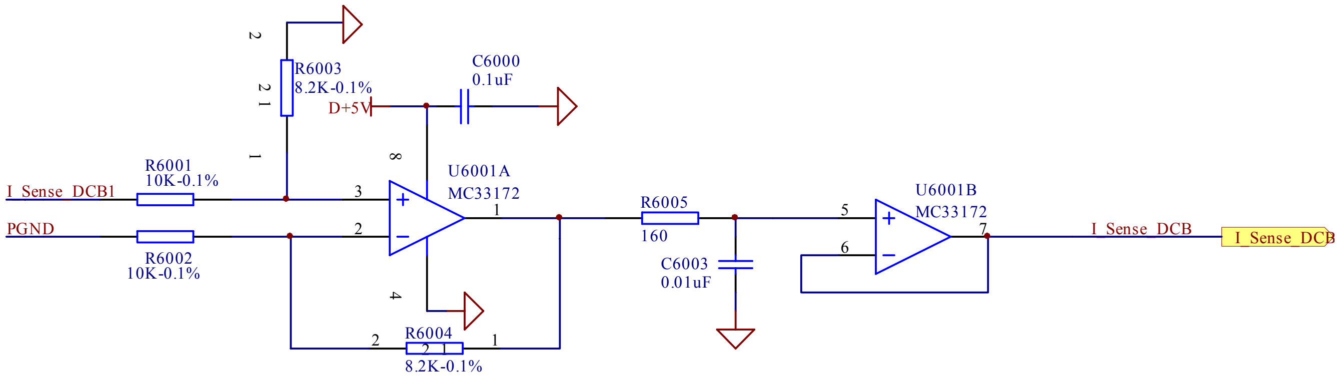

Figure 6-5. Bus Link Current Sample Circuit

C. Phase Current Sensor

The stator flux and electromagnetic torque can be derived from two phase currents and voltages. The use of a Hall current transducer will sharply increase the cost, and two channel differential amplifiers are used as the Analog-to-Digital Converter (ADC) to sample phase currents as shown in **Figure 6-6**. The SVPWM is employed. The state in which all bottom switches are turned on and upper switches are turned off is defined as state 0, and the corresponding equivalent topology is depicted in **Figure 6-6** (b). The sample is triggered at state 0, shown in **Figure 6-6** (c). In this way, two phase currents can be derived through the differential amplifier channels. The spot worth consideration is that a certain margin Δ should be maintained between the circle track formed by the reference voltage vector $\vec{V}_{ref}$ and the inscribed circle of the hexagon shaped by the six base vectors as described in **Figure 6-6** (a), especially at the high speed range.

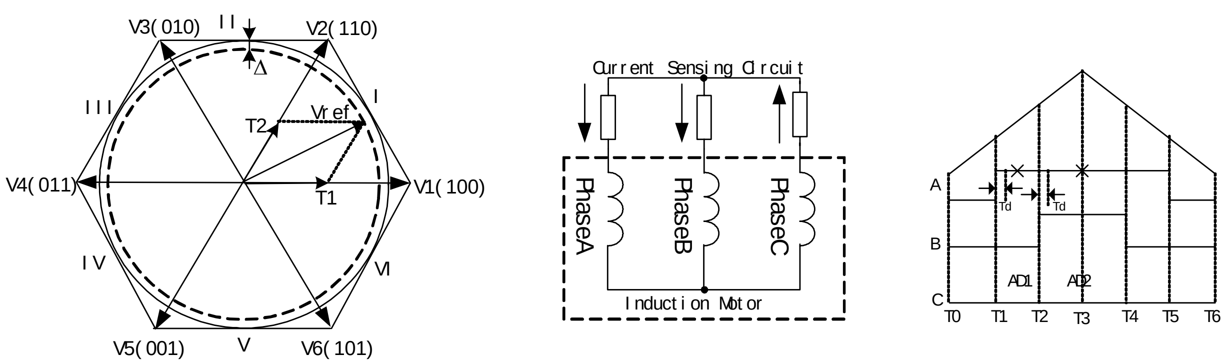

(a) SVPWM **(b) Equivalent Topology** **(c) Sample Time**

Figure 6-6. Methods to Detect Phase Currents

D. Power Supply Stage

The power supply stage provides a high-voltage DCBus +5V power supply for the drive and auxillary power and +15V for the 56F8013, high-voltage drivers and amplifiers. A topswitch generates auxiliary power supply of +15V for both the ICs and the IPM. PFC is employed to make the input current trace the input voltage and to reduce the EMI.

E. Protection Circuit

To improve the system safety level, overcurrent and overvoltage in the bus link detection and protection are introduced into the system, illustrated in **Figure 6-7**. The signal generated by the circuit “IPMLOCK” will be connected to the IPM’s drive IC (74HC244) and to the 56F8013’s fault pin. When a fault is generated, the IPMLOCK signal draws to high level. On the one hand, the IPMLOCK will disable the 74HC244 and the PWM signals won’t pass through; on the other hand, the IPMLOCK signal will drive the 56F8013’s fault0 pin, and the 56F8013 will block the PWM signal instantly.

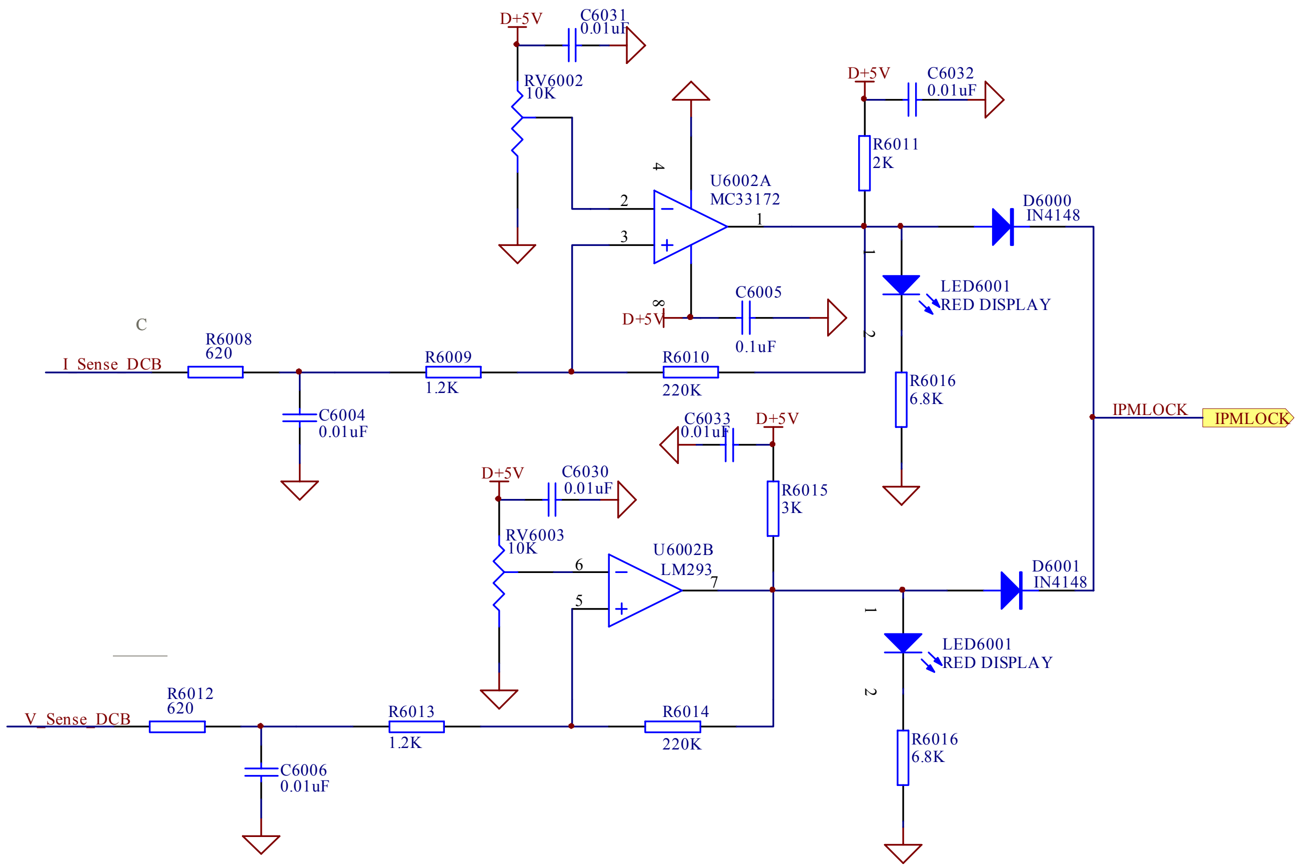

Figure 6-7. Protection Circuit

6.4 PFC Hardware Design

The topology of the main circuit is a boost circuit. One signal, output bus voltage *DC_bus,* is sampled and sent to the 56F8013.

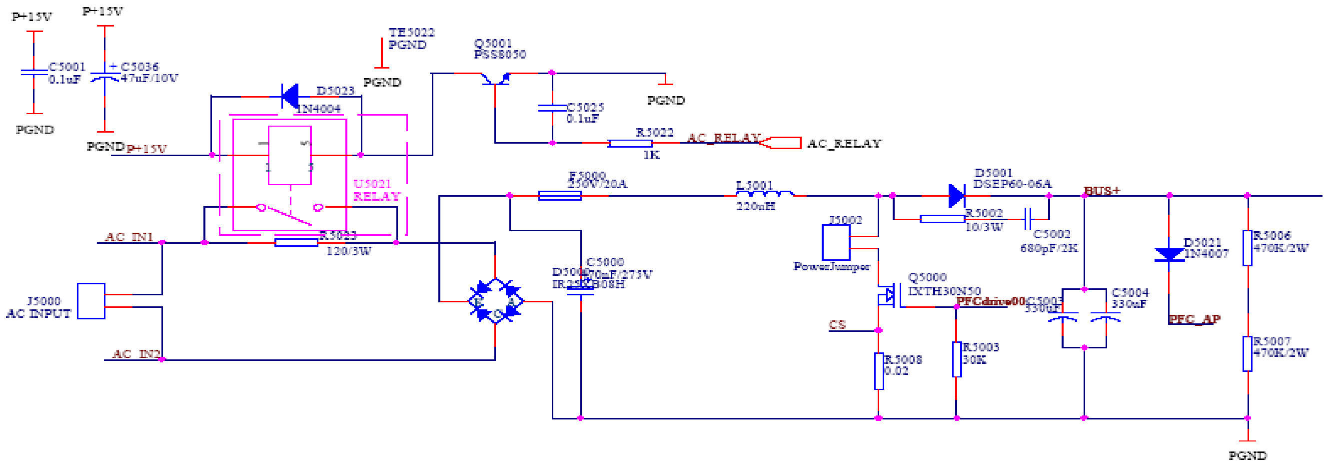

Figure 6-8. Main PFC Circuit

6.4.1 Drive Circuit Hardware Design

IC IR2125, a simple and reliable gate drive circuit based on a current-limiting single channel driver, is used; it is shown in **Figure 6-9**.

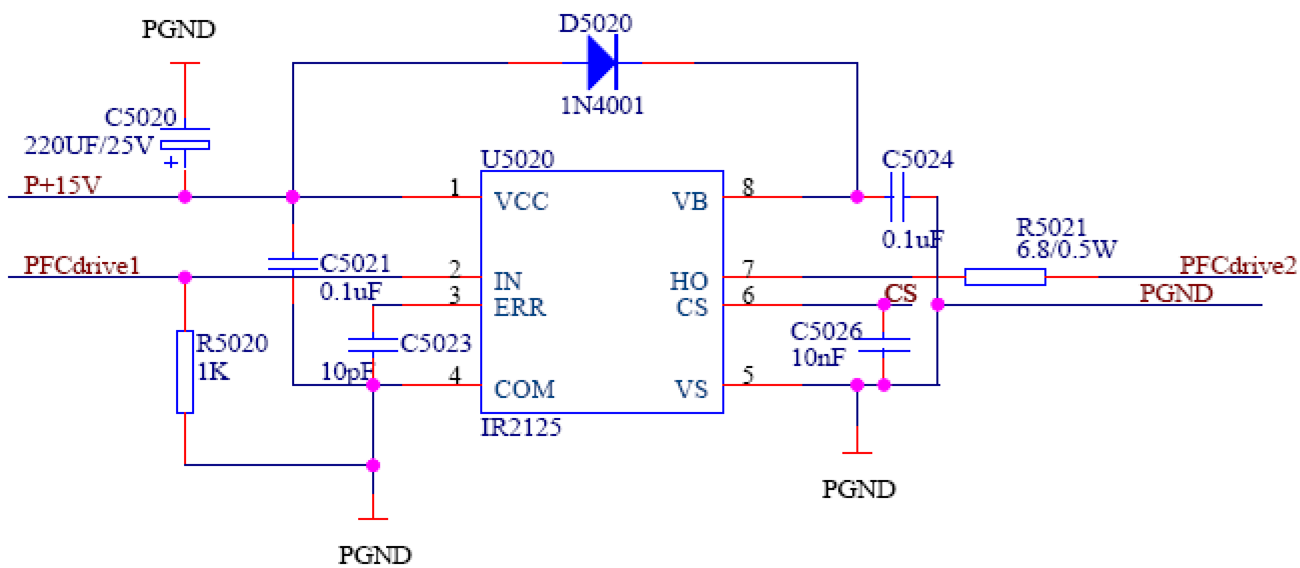

Figure 6-9. PFC Drive Circuit

6.4.2 Sample Circuit Hardware Design

The output bus voltage, V_{bus}, sample circuit is shown in **Figure 6-10**. A simple voltage divider is used for the bus voltage sample.

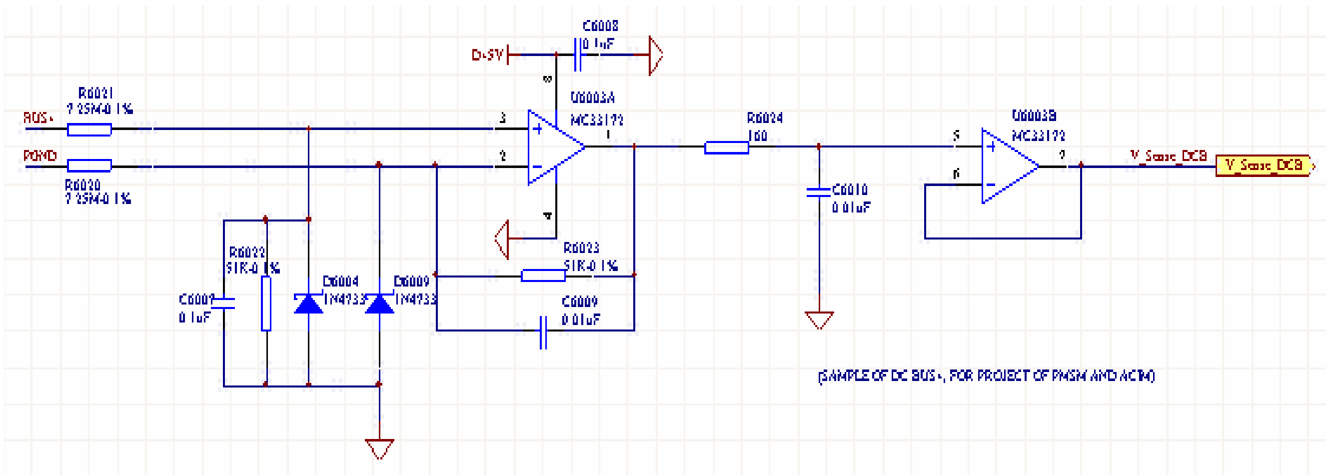

Figure 6-10. PFC Sampling Circuit

6.5 Detailed Motherboard Configurations for ACIM

The motherboard shown in **Figure 6-2** comprises a high-voltage power stage, a sensor stage, a protection circuit and PFC. It is a general board which can be used for ACIM, BLDC and PMSM after simple configuration with resistances and jumpers.

Configurations for the ACIM are shown in **Figure 6-11**; shorten circuits for the jumpers circled in red.

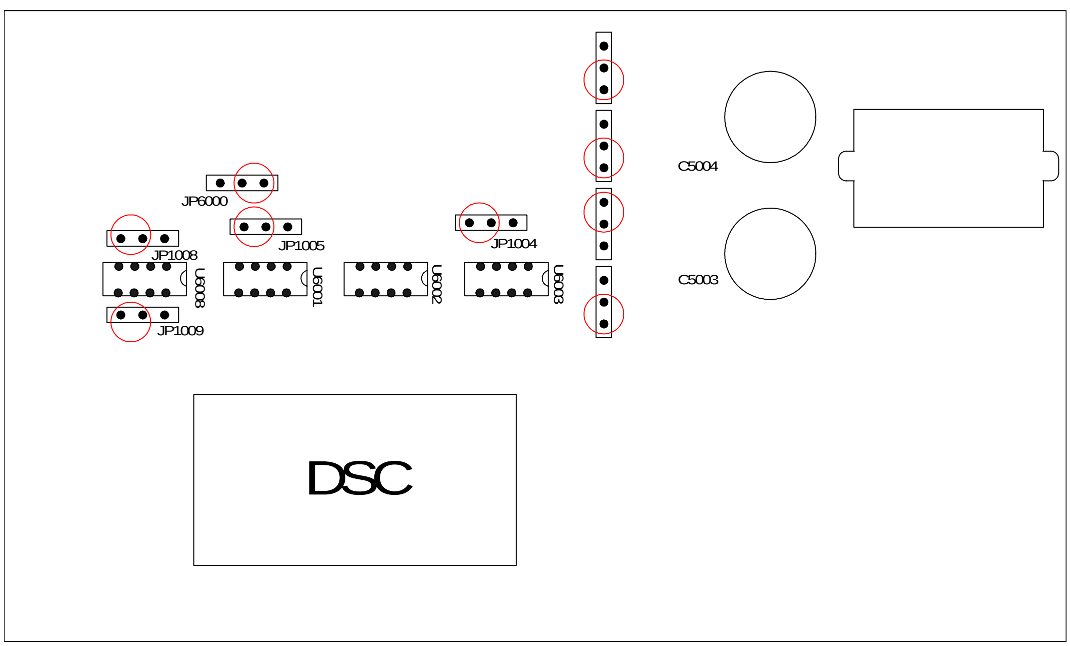

Figure 6-11. ACIM Jumper Configuration

Table 6-1 details the configurations of the 56F8013 resources used in the system and the corresponding variables used in the software.

Table 6-1. Configuration of the 56F8013's Resources

Target Variables	56F8013 Resources	Software Resources	
DCBus Voltage: V_sense_DCB	ANB1 (PC5)	sample3	AD_VDC
Uphase Current Sample: I_sense_U	ANA1 (PC1	sample0	AD_iA
Vphase Current Sample: I_sense_V	ANA0 (PC0)	sample1	AD_iB
DCBus Current Sample: I_Sense_DCB	ANB0 (PC4	sample4	AD_iDC
Relay: AC_RELAY	PB5		
OPEN: OPEN	PB2		
DACCLK	PB0		
DACDATA	PB3		
DACEN	PB1		
TXD	PB7		
RXD	PB6		
FAULT0	PA6		

Chapter 7
Software Design

This section describes the design of the drive's software blocks. The software will be described in terms of:

- Control Algorithm Data Flow
- State Diagram

7.1 Data Flow

The drive requires the software to gather and process values from the user interface and generate 3-phase PWM signals for inverter. The control algorithm contains the processes, described in the following sections.

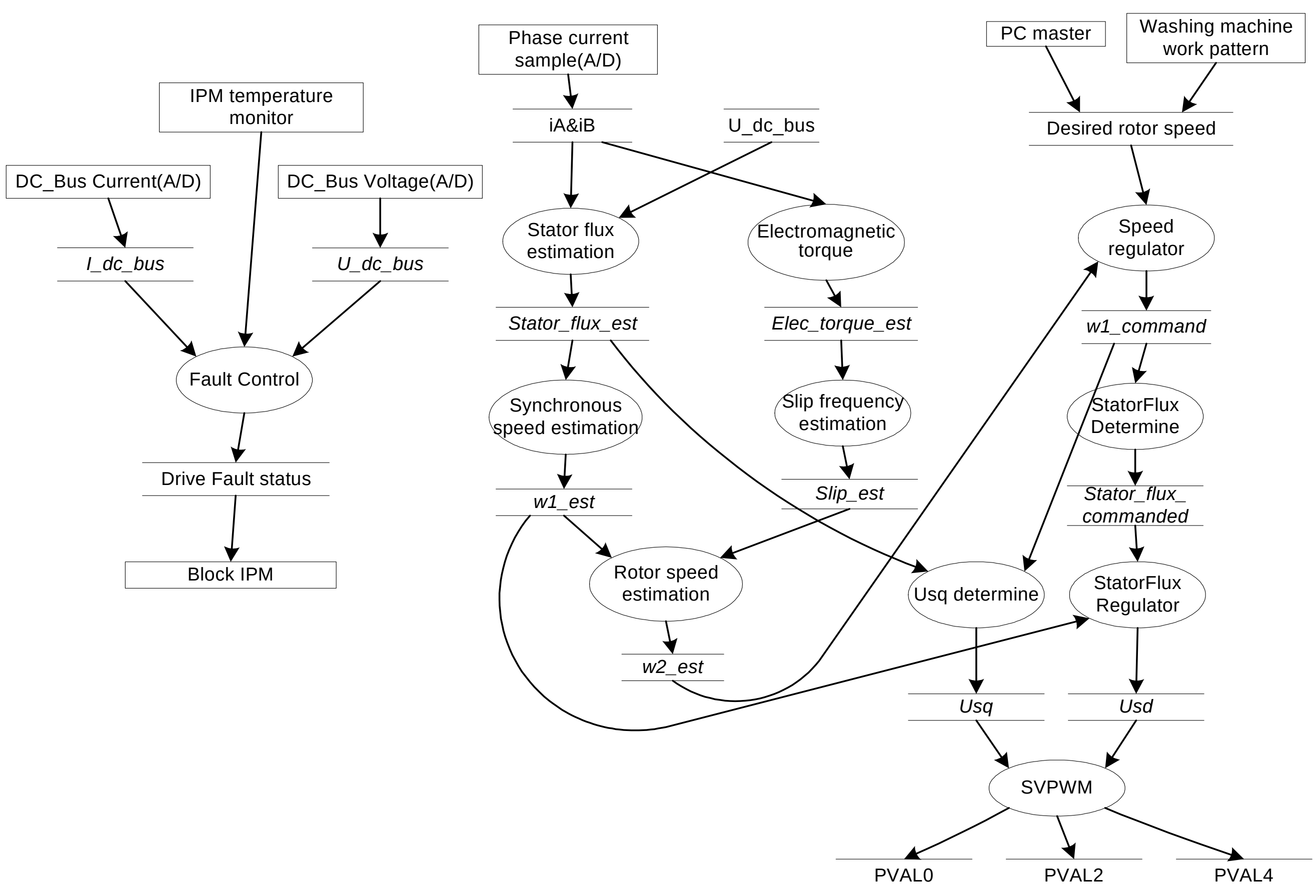

Figure 7-1. Data Flow

7.2 Stator Flux Estimation

Estimating stator flux is one of the algorithm's key tasks. Using the phase voltages and phase currents, an estimation of stator flux can be derived from the stator flux model. Generally, the stator flux based on the voltage model is determined by **Equation 7-1**.

$$\vec{\Psi}_s = \frac{\vec{U}_s - R_s\vec{i}_s}{j\omega_1} = \frac{\vec{E}}{j\omega_1} = \frac{E}{\omega_1}e^{j(\angle\vec{E}-90^\circ)}$$

Eqn. 7-1

Where:
$\vec{E}$ is the back EMF
E is the magnitude of $\vec{E}$
$\angle E$ is the phase of $\vec{E}$

The pure integral of back EMF involves the drift and saturation problems due to initial condition and DC offset. The Low-Pass Filter (LPF) is employed to replace the pure integral as shown in **Figure 7-2**.

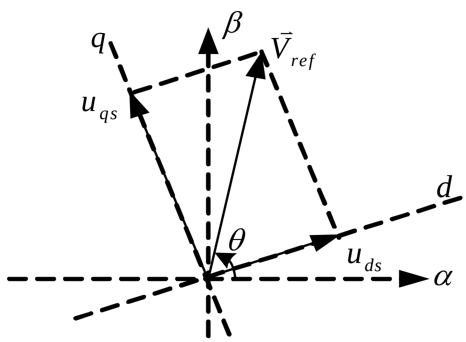

Figure 7-2. Stator Reference Voltage $\vec{V}_{ref}$

$$\vec{\Psi}'_s = \frac{\vec{E}}{j\omega_1 + \omega_c} = \frac{E}{\sqrt{\omega_1^2 + \omega_c^2}}e^{j(\angle\vec{E} - \arctan\frac{\omega_1}{\omega_c})}$$

Eqn. 7-2

Where:

ω_c is the cutoff frequency of the LPF in radians per second

As expected, when $\omega_1 >> \omega_c$:

$$\arctan\frac{\omega_1}{\omega_c} \approx 90^\circ$$

Eqn. 7-3

$$\sqrt{\omega_1^2 + \omega_c^2} \approx \omega_1$$

Eqn. 7-4

In this case, the LPF estimator approaches the pure integrator estimator. But when the cut-off frequency, ω_c, is close to the synchronous ω_1, errors occur, so a correction factor, $\overline{G}$, is used to minimize the errors.

$$\vec{\Psi}'_s \vec{G} = \vec{\Psi}_s \qquad \text{Eqn. 7-5}$$

Equation 7-6 can be deduced:

$$\vec{G} = \frac{\sqrt{\omega_1^{\,2} + \omega_c^{\,2}}}{\omega_1} e^{j(\arctan\frac{\omega_1}{\omega_c} - 90^\circ)} = G(\omega_1) e^{j\rho(\omega_1)} \qquad \text{Eqn. 7-6}$$

The improved stator flux observer channel is shown in Figure 7-3.

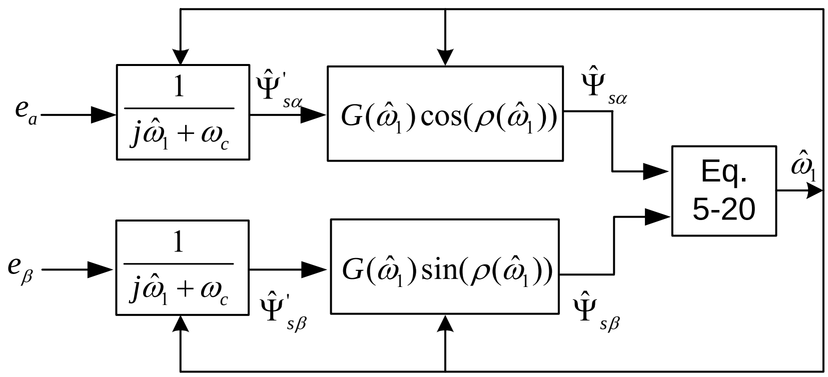

Figure 7-3. Improved Stator Flux Estimation Channel

7.3 Electromagnetic Torque

Electromagnetic torque can be estimated from stator flux and stator current and can be determined as shown in Equation 7-7.

$$T_e = -\Psi_{s\beta} i_{s\beta} + \Psi_{s\alpha} i_{s\beta} \qquad \text{Eqn. 7-7}$$

7.4 Rotor Speed Estimation

A speed sensorless induction motor drive is a trend in today's low cost variable speed applications. Due to the cost and maintenance required by a speed transducer, speed sensorless technology is drawing more attention. For convenience, this application assumes a simple method to estimate rotor speed, described in Section 5.6.

7.5 Stator Flux Determination

The motor will get an optimum transformation from energy produced by magnetic field compared to that produced mechanically when it works at the point of the flux linkage curve. At the high speed range, however, the flux should be weakened to reach a high speed. Therefore, the electrical machine should maintain the flux below the rated speed range, and the flux should be weakened at the high speed range. The flux should be regulated depending on the rotor speed.

7.6 Space Vector Pulse Width Modulation (SVPWM)

Space Vector Modulation (SVM) can directly transform the stator voltage vectors from an α, β-coordinate system to Pulse Width Modulation (PWM) signals (duty cycle values).

The standard technique for output voltage generation uses an inverse Clarke transformation to obtain 3-phase values. Using the phase voltage values, the duty cycles needed to control the power stage switches are then calculated. Although this technique gives good results, space vector modulation is more straightforward and realized more easily by a digital signal controller.

7.7 Fault Control

From the consideration of the cost control, optocoupler is not used in this system. The fault control process and its hardware should be designed to provide a solid protection against damage. In this application, due to the high complex of the pins, the fault1 to fault3 input pins are coupled with the PWM output pads. Only fault0 is valid for the detection of the rising edge generated by the fault signals. The overcurrent, overvoltage and overheat protections are merged together with the OR relation; that is, if any of them occur, the pin Fault0 will catch the edge and the fault process will dominate all resources and disable the PWM output pads. The routine will trap into the Interrupt Service Routine (ISR) once the fault occurs.

7.8 PFC Software Design

Power Factor (PF) is defined as the ratio between real power and apparent power of AC input. Assuming input voltage is a perfect sine wave, PF can be defined as the product of current distortion and phase shift. Consequently, the PFC circuit's main tasks are:

- Controlling inductor current, making the current sinusoidal and the same phase as input voltage
- Controlling output voltage, insuring the output voltage is stable.

  The PFC main current needs two closed loops to control the circuit:

  — The voltage loop is the outer loop, which samples the output voltage and controls it to a stable level

  — The current loop is the inner loop, which samples inductor current and forces the current to follow the standard sinusoidal reference in order to reduce the input harmonic current

The system in this application is based on current Discontinuous Current Mode (DCM), in which there is only a voltage loop. DCM can make the current both sinusoidal and the same phase as input voltage.

PI loop control is widely used in industry control because of its simplicity and reliability. In this application, the voltage loop adopts PI regulator arithmetic.

These assumptions simplify analysis:

- Input current follows reference perfectly, which is proportional to the input voltage
- There is no additional power depletion in the circuit; power efficiency is 1
- Output power is constant

Figure 7-4. Simple PFC Mode

The function for output voltage:

$$\begin{cases} Uv(n) = K0v \times Ev(n) + Iv(n-1) \\ Iv(n) = Iv(n-1) + K1v \times Ev(n) + Kcorrv \times Epiv \\ Epiv = Usv - Uv(n) \end{cases}$$

$$Usv = \begin{cases} Uv_{\max} & when Uv(n) \geq Uv_{\max} \\ Uv_{\min} & when Uv(n) \leq Uv_{\min} \\ Uv(n) & else \end{cases}$$

Uv(n)	=	the result of PI unit
Ev(n)	=	input error
Iv(n)	=	integral unit
K0v	=	proportional constant
K1v	=	integral constant
Kcorrv	=	resistant saturation constant
Usv	=	result of voltage loop after limit
iUv_{max}	=	maximum of voltage loop
Uv_{min}	=	minimum of voltage loop

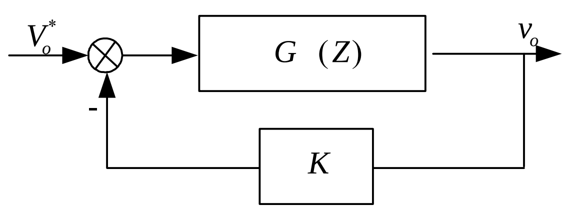

Figure 7-5. Discrete Voltage Loop Structure

Chapter 8
JTAG Simulation and SCI Communication

There are abundant software and hardware resources for JTAG simulation and communication in the 56F8013 device. With these resources, a 56F8013-based motor system can accomplish mixed communication functions, such as JTAG debug and SCI interface, between the power module and PC. Isolation is necessary between power electronics and microelectronics in the power system for safety.

The communication system consists of two parts:

- JTAG circuit, designed with for debugging and programming the 56F8013
- SCI circuit, designed for background communication from the PC; power management and supervision can be realized conveniently

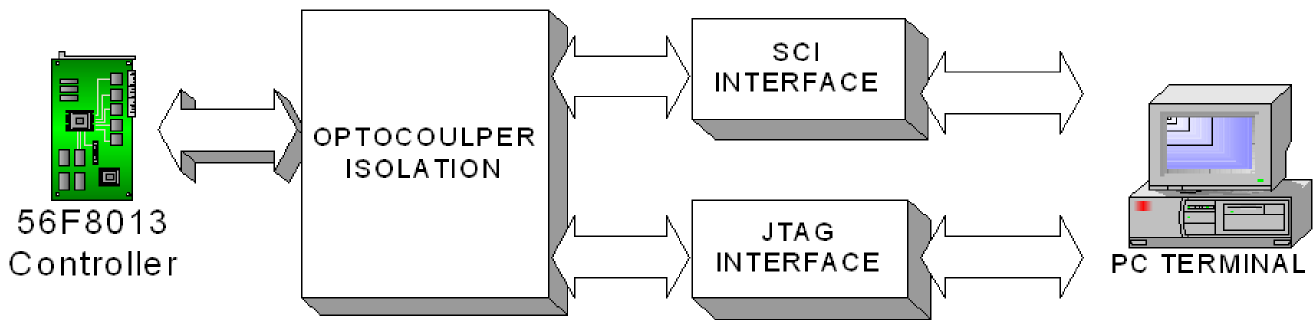

Figure 8-1. Communication Board's Frame Figure

8.1 JTAG Simulation Function

Because the 56800E core integrates the JTAG/EOnCE function, the 56F8013 can be debugged and programmed through the parallel port by a simple interface circuit without any special emulator. The debug function is provided by JTAG interface.

The power main circuit must be removed to ensure safety. During debugging, the connection for main power circuit should be cut off by disconnecting the J5000 connector on power board; see **Figure 8-2**.

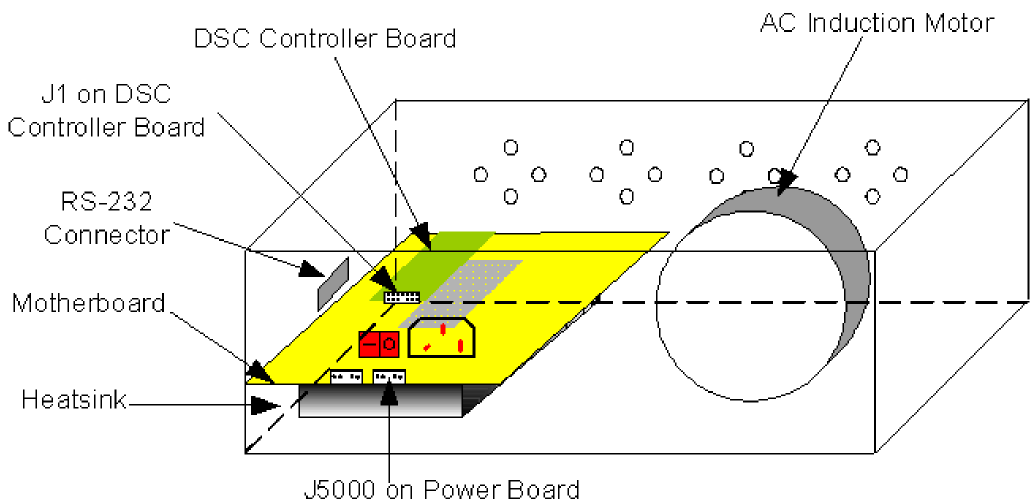

Figure 8-2. System Diagram

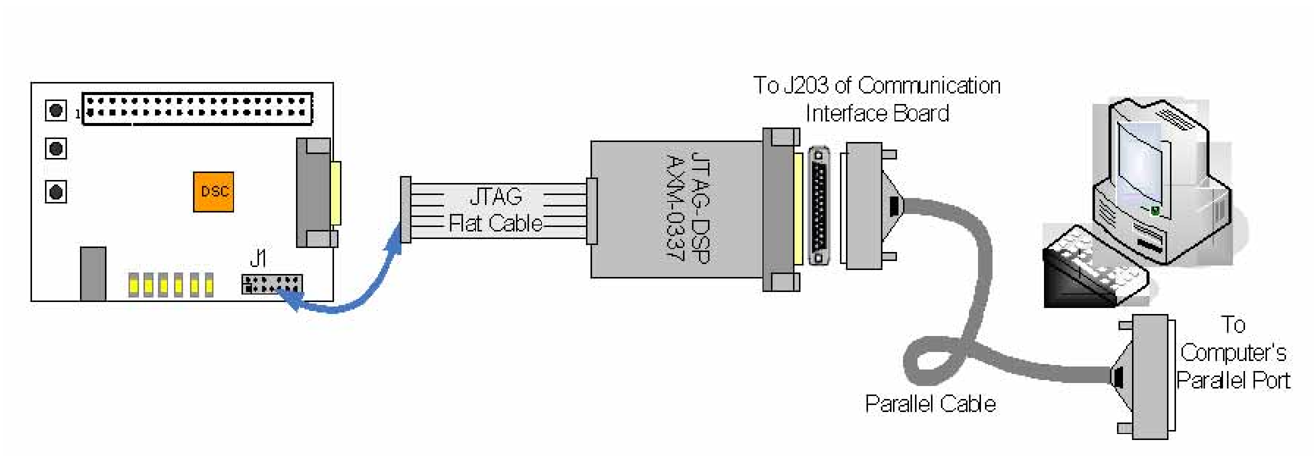

Figure 8-3. Connections for JTAG

As shown in **Figure 8-3**, the JTAG flat cable is connected to the 56F8013's J1. A parallel cable links the JTAG to PC's parallel port.

CAUTION
Disconnect J5000 in the Power Board before debugging or refreshing the control program. Otherwise, damage to or invalidation of the demo, or even electrical shock, can occur. Debugging or refreshing the control program should only be done by experienced personnel.

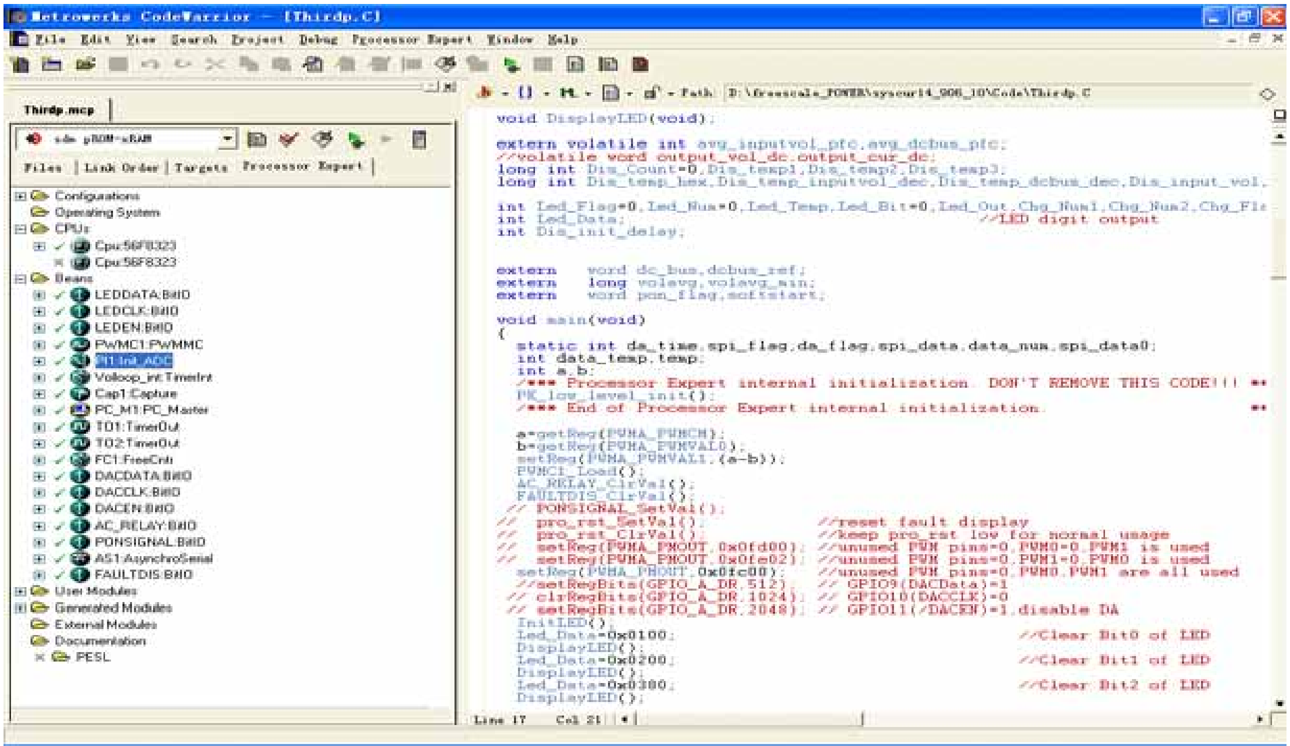

Figure 8-4. CodeWarrior Development Tool Interface

CodeWarrior IDE is necessary to debug software and refresh the program; version 7.0 or later is recommended. Figure 8-4 shows the software interface. Details about installation and use can be found in the CodeWarrior documentation.

8.2 SCI Communication Function

Connections for SCI communication are shown in Figure 8-5. A serial cable links the RS-232 connector on the demonstration board to the PC’s serial port.

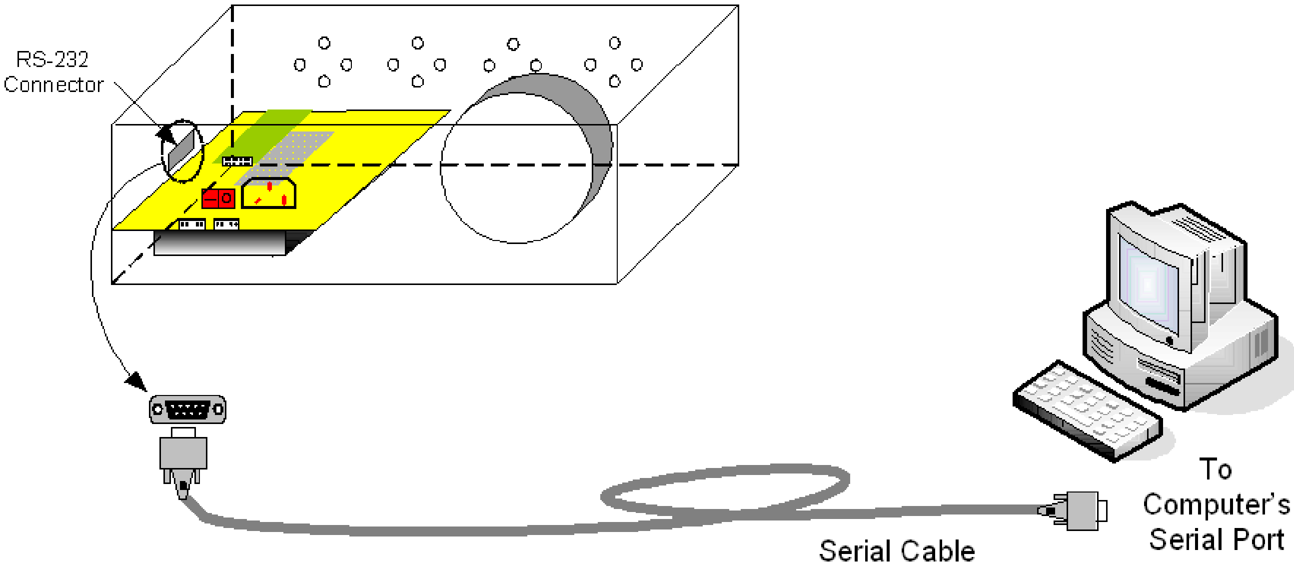

Figure 8-5. SCI Communication Connections

The PC Master software tool can be used for development and control of the application. Details about installation and use of PC master software can be found in the CodeWarrior tool.

Chapter 9
Operation

This section offers brief instructions on operating the ACIM application.

9.1 Switch-on

Follow these steps to start the ACIM application:

1. Make sure the power switch is on the POWEROFF state, then put the plug in a wall socket
2. Switch the appliance on by pressing down the POWERON button.

   The 56F8013 starts the main power, and the ACIM begins to work

9.2 During Operation

1. LEDs on controllers can display system information
   — LED 1 displays the operating mode
   — LED 2 displays the rotation speed
2. SCI communication provides background supervision for the power module
   — SCI baud rate configuration: 4800 BPS
3. Debug function is provided by the JTAG interface

   See Caution, **Section 8.1** and **Section 9.4**
4. To ensure the demo plate coupled on the shaft of the motor will not fly out, be sure the upper cover of the box is closed

9.3 Switch-off

To turn the application off, follow these steps:

1. Switch off the POWERON Button
   — The 56F8013 cuts off the main power and the bus voltage is decreased
2. Unplug the power line.
   — The controller is powered off, and system is switched off

9.4 Cautions

To ensure safety, take care when:

1. Pressing the power switch to 1 on the unit after the power line is plugged in during the switch-on process
2. Pressing the power switch to 0 before power line is unplugged during the switch-off process
3. Debugging
   Before beginning the debug process, cut off power to the main power circuit by disconnecting the J5000 connector on the Power Board

Appendix A
Schematics

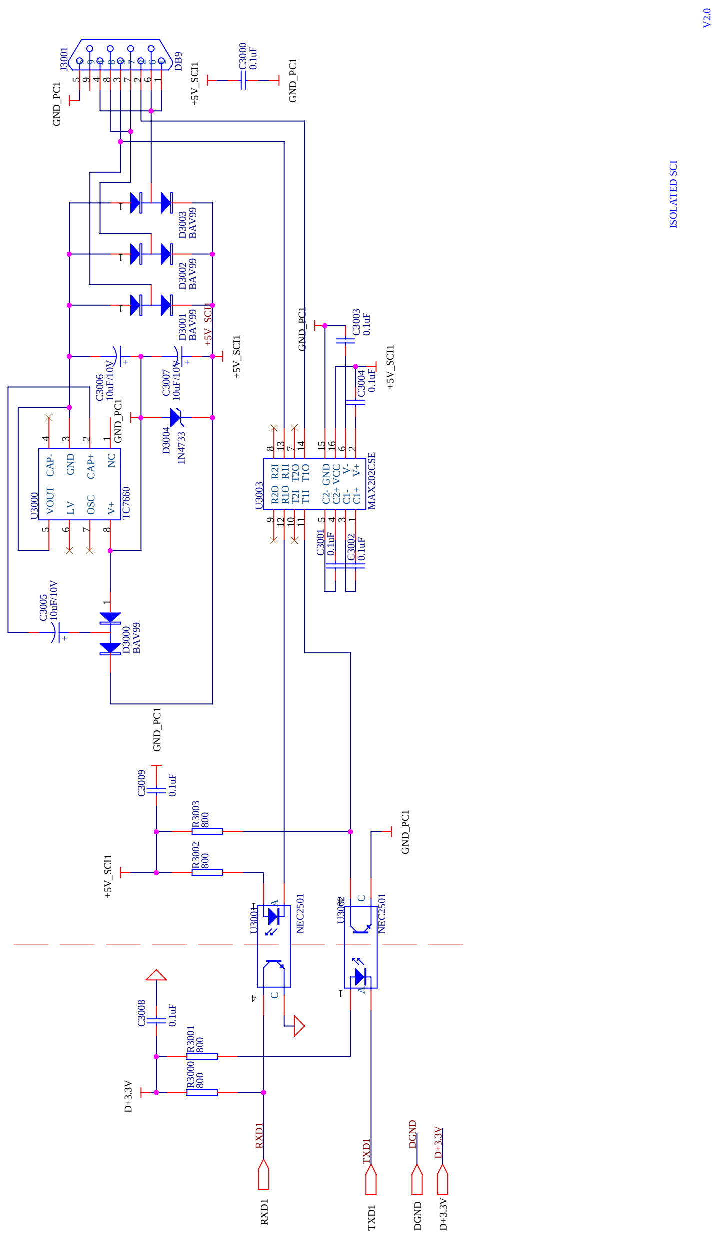
J3001
DB9
GND_PC1
+5V_SCI1
C3000
0.1uF
D3003
BAV99
D3002
BAV99
D3001
BAV99
C3006
10uF/10V
C3007
10uF/10V
D3004
1N4733
U3000
TC7660
C3005
10uF/10V
D3000
BAV99
U3003
MAX202CSE
C3003
0.1uF
C3004
0.1uF
C3001
0.1uF
C3002
0.1uF
C3009
0.1uF
R3003
800
R3002
800
U3001
NEC2501
U3002
NEC2501
C3008
0.1uF
R3001
800
R3000
800
D+3.3V
RXD1
TXD1
DGND
ISOLATED SCI
V2.0

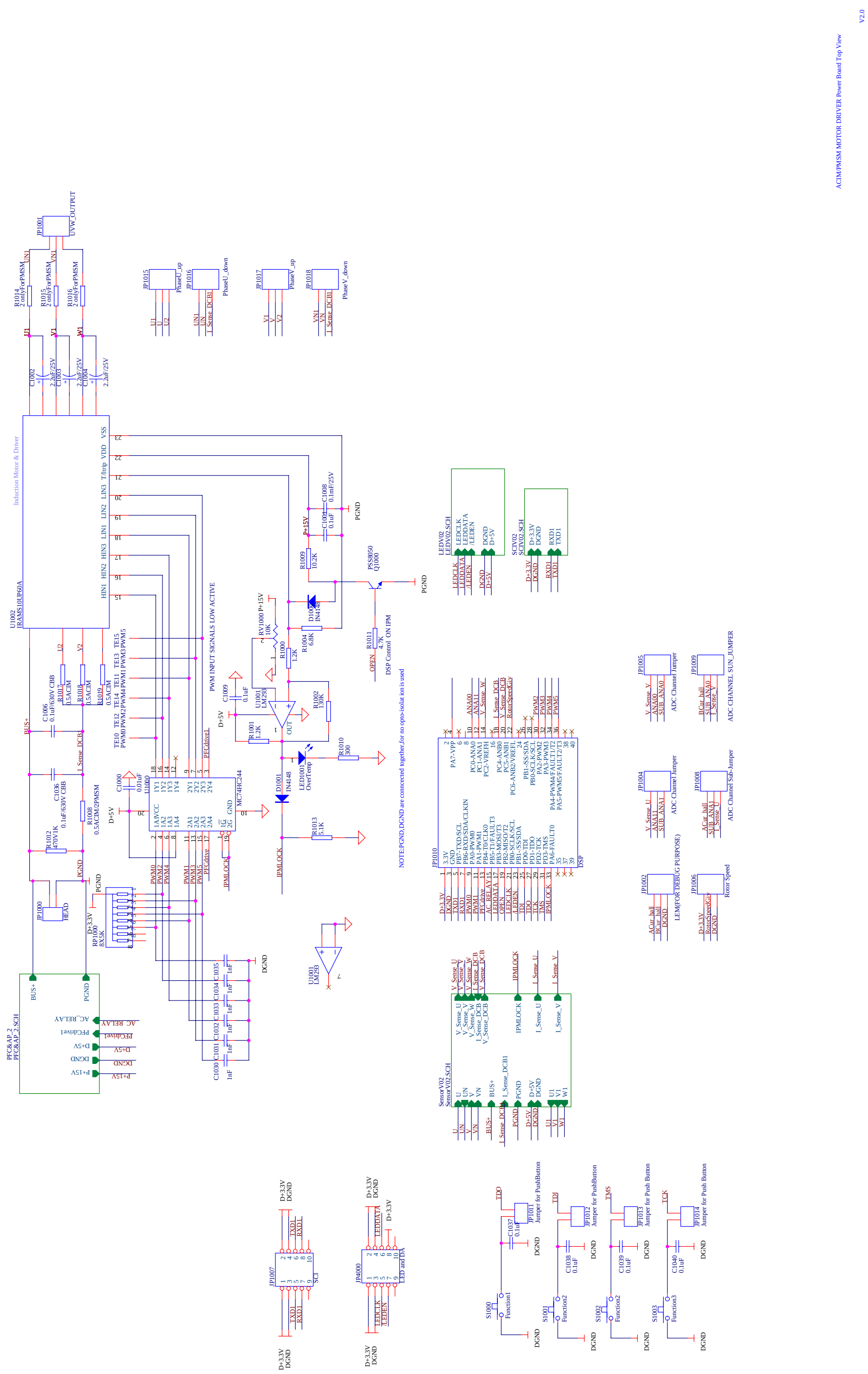

Schematics, Rev. 1

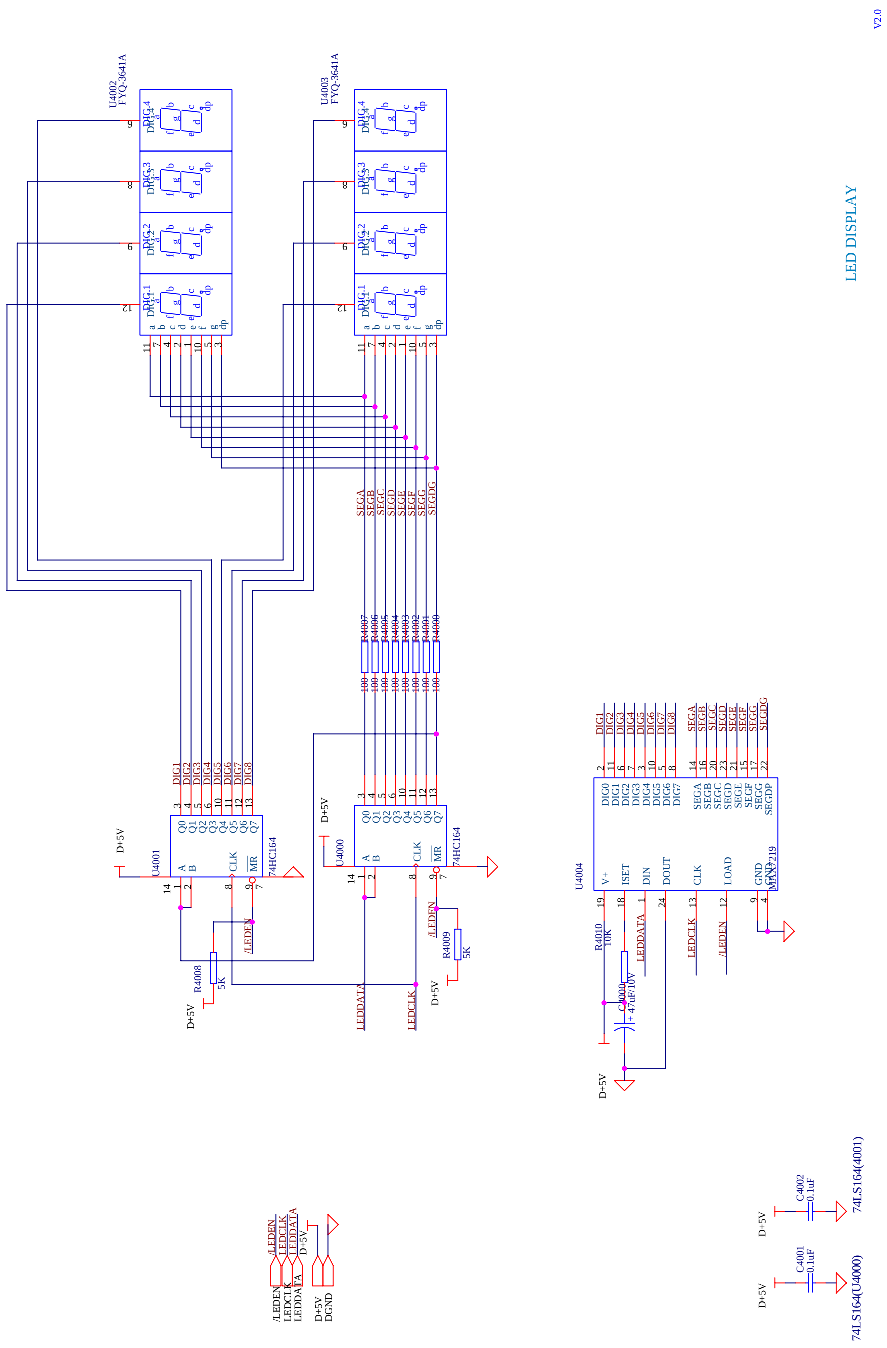
LED DISPLAY
V2.0

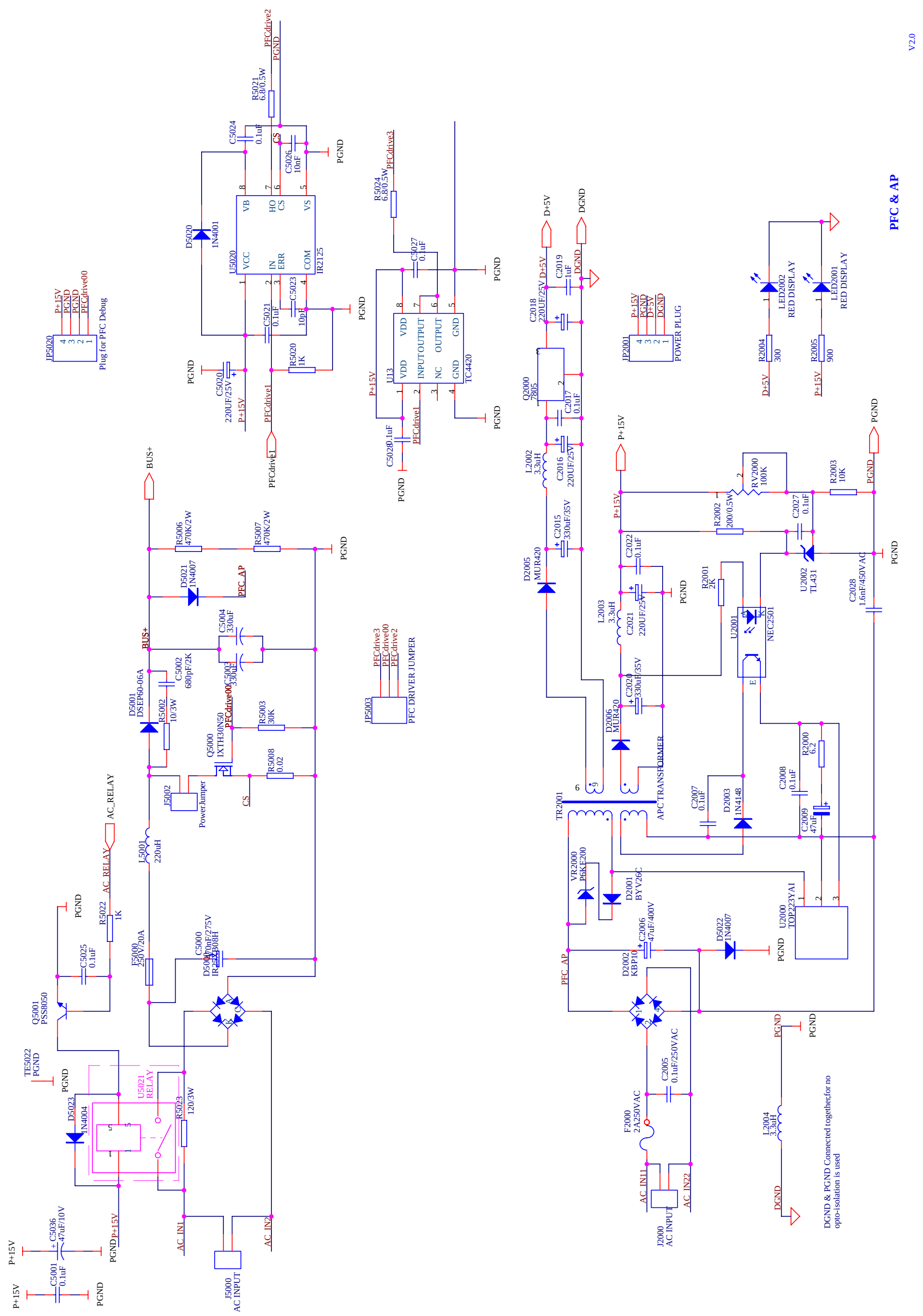

Schematics, Rev. 1

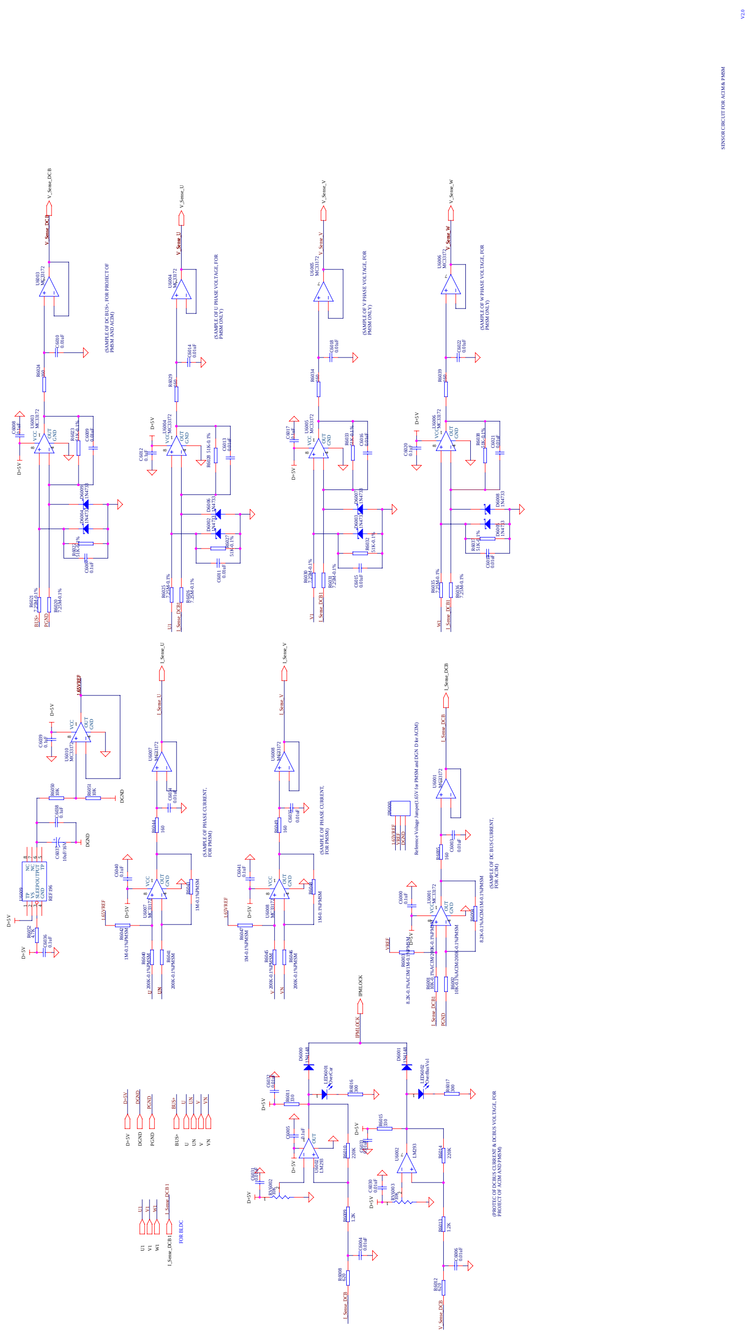

Appendix B
ACIM Bill of Materials

Designator	Description	Footprint	Quantity
C1000, C6003, C6004,C6006, C6009, C6010, C6011, C6013, C6014, C6015, C6016, C6018, C6019, C6021, C6022, C6030, C6031, C6032, C6033, C6034, C6035	0.01 µF	RAD-0.1	21
C1001, C1009, C1037, C1038, C1039, C1040, C2007, C2008, C2017, C2022, C2027, C3000, C3001, C3002, C3003, C3004, C3008, C3009, C4001, C4002, C5001, C5021, C5024, C5025, C5027, C5028, C6000, C6005, C6007, C6008, C6012, C6017, C6020, C6036, C6038, C6039, C6040, C6041	0.1 µF	RAD-0.1	38
C1002, C1003	2.2 µF / 25 V	RB2.5/5	2
C1006, C1036	0.1 µF / 630V CBB	RAD15/18/6	2
C1008	0.1 mF / 25V	RB2.5/6	1
C1030, C1031, C1032, C1033, C1034, C1035	1 nF	RAD-0.1	6
C2005	0.1 uF / 250VAC	RAD15/18/6	1
C2006	47 µF / 400V	RB10/22.4	1
C2009	47 µF	RB2.5/5	1
C2015, C2020	330 µF / 35V	RB5/10	2
C2016, C2018, C2021, C5020	220 µF / 25V	RB3/8	4
C2019	1 µF	RAD-0.2	1
C2028	1.6 nF / 450VAC	RAD-0.4	1
C3005, C3006, C3007	10 µF / 10V	RB2.5/5	3
C4000, C5036	47 µF / 10V	RB2.5/5	2
C5000	470 nF / 275V	RAD22/26/9	1
C5002	650 pF / 2K	RAD-0.2	1
C5003, C5004	330 µF	RB10/30	2
C5023	10 pF	RAD-0.1	1
C5026	10 nF	RAD-0.1	1

Designator	Description	Footprint	Quantity
C6037	10 µF / 16V	RB2.5/5	1
D1000, D1001	IN4148	DIODE-0.4	2
D2001	BYV26C	DIODE-0.4	1
D2002	KBP10	KBP19	1
D2003	IN4148	DIODE-0.4	1
D2005, D2006	MUR420	DIODE-0.5	2
D3000, D3001, D3002, D3003	BAV99	SOT-23	4
D3004	IN4733	DIODE-0.4	1
D5000	IR25XB08H	IR25XB	1
D5001	DSEP60-06A	TO247AD	1
D5020	IN4001	IN4007	1
D5021, D5022	IN4007	IN4007	2
D5023	IN4004	IN4004	1
D6000, D6001	IN4148	DIODE-0.4	2
D6002, D6003, D6004, D6005, D6006, D6006, D6008, D6009	IN4733	DIODE-0.4	8
F2000	Fuse 2A 250 VAC	FUSE20/5/7	1
F5000	Fuse 250V / 20A	FUSE20/5/7	1
J2000, J5000	AC INPUT Connectors	CON5/3.96	2
J3001	DB9 Connector	DB9/M	1
J5002	Power Jumper	CON2/3.96	1
JP1000	Jumper HEAD	CON5/3.96	1
JP1001	Jumper UVW_OUTPUT	UVW	1
JP1002	Jumper LEM (For Debug Purpose)	HDR1X3	1
JP1004, JP1005	ADC Channel Jumper	HDR1X3	2
JP1006	Jumper Rotor Speed	HDR1X3	1
JP1007	Jumper SCI	IDC10	1
JP1008	ADC Channel Jumper	HDR1X3	1

Designator	Description	Footprint	Quantity
JP1009	ADC Channel Jumper	HDR1X3	1
JP1010	DSC Demo Board Connector	HDR2X20	1
JP1011, JP1012, JP1013, JP1014	Jumper for Push Button	HDR1X2	4
JP1015	Jumper PhaseU_up	HDR1X3	1
JP1016	Jumper PhaseU_down	HDR1X3	1
JP1017	Jumper PhaseV_up	HDR1X3	1
JP1018	Jumper PhaseV_down	HDR1X3	1
JP2001	Jumper PowerPlug	HDR1X4-5	1
JP4000	LED and DA	IDC10	1
JP5003	PFC Driver Jumper	HDR1X3	1
JP5020	Jumper Plug for PFC Debug	HDR1X4	1
JP6000	Reference Voltage Jumper (1.65 for PMSM and DGND for ACIM)	HDR1X3	1
L2002, L2003	3.3 µH	IND3.3u	2
L2004	3.3 µH	IND	1
L5001	220 µH	IND_PFC	1
LED1001	LED OverTemp	LEDA	1
LED2001, LED2002	RED LED DISPLAY	LEDA	2
LED6001	LED OverCur	LEDA	1
LED6002	LED OverBusVol	LEDA	1
Q1000, Q5001	PSS8050	TO-92A	2
Q5000	IXTH30N50	TO247AC	1
R1000, R1001	1.2K Ohm	AXIAL-0.4	2
R1002	130K Ohm	AXIAL-0.4	1
R1004	6.8K Ohm	AXIAL-0.4	1
R1008	6.8K Ohm	AXIAL-0.4	1

Designator	Description	Footprint	Quantity
R1009	10.2K	AXIAL-0.4	1
R1010	300 Ohm	AXIAL-0.4	1
R1011	4.7K Ohm	AXIAL-0.4	1
R1012	470V 1K Ohm	VVR	1
R1013	5.1K Ohm	AXIAL-0.4	1
R1014, R1015, R1016	2 Ohm (PMSM)	SHANT-0.5	3
R1017, R1018, R1019	0.5 Ohm (ACIM)	SHANT-0.5	3
R2000	6.2 Ohm	AXIAL-0.4	1
R2001	2K Ohm	AXIAL-0.4	1
R2002	200 Ohm / 0.5W	AXIAL-0.5	1
R2003	10K Ohm	AXILA-0.4	1
R2004	300 Ohm	AXIAL-0.4	1
R2005	900 Ohm	AXIAL-0.4	1
R3000, R3001, R3002, R3003	800 Ohm	AXIAL-0.4	4
R4000, R4001, R4002, R4003, R4004, R4005, R4006, R4007	100 Ohm	AXIAL-0.4	8
R4008, R4009	5K Ohm	AXIAL-0.4	2
R4010, R6050, R6051	10K Ohm	AXIAL-0.4	3
R5002	10 Ohm / 3W	R2WV	1
R5003	30K Ohm	AXIAL-0.4	1
R5006, R5007	470K Ohm / 2W	R2WV	2
R5008	0.02 Ohm	SHANT-0.2	1
R5020, R5022	1K Ohm	AXIAL-0.4	2
R5021, R5024	6.8 Ohm / 0.5W	AXIAL-0.5	2
R5023	120 Ohm / 3W	RXWV	1
R6001, R6002	10K Ohm - 0.1% (ACIM) / 200K Ohm - 0.1% (PMSM)	AXIAL-0.4	2
R6003, R6004	8.2K Ohm -0.1% (ACIM) / 1M Ohm -0.1% (PMSM)	AXIAL-0.4	2

Designator	Description	Footprint	Quantity
R6005, R6024, R6029, R6034, R6039, R6044, R6049	160 Ohm	AXIAL-0.4	7
R6008	620 Ohm	AXIAL-0.4	1
R6009, R6013	1.2K Ohm	AXIAL-0.4	2
R6010, R6014	220K Ohm	AXIAL-0.4	2
R6011, R6015	330 Ohm	AXIAL-04	2
R6012	620 Ohm	AXIAL-04	1
R6016, R6017	300 Ohm	AXIAL-04	2
R6020, R6021, R6025, R6026, R6030, R6031, R6035, R6036	7.25M Ohm - 0.1%	AXIAL-04	8
R6022, R6023, R6027, R6028, R6032, R6033, R6037, R6038	51K Ohm - 0.1%	AXIAL-04	8
R6040, R6041, R6045, R6046	200K Ohm - 0.1% (PMSM)	AXIAL-04	4
R6042, R6043, R6047, R6048	1M Ohm - 0.1% (PMSM)	AXIAL-04	4
R6052	4.7K Ohm	AXIAL-04	1
RP1000	Resistor Pack 8 X 5K Ohm	SIP9	1
RV1000, RV6002, RV6003	10K Ohm	VRESLV	3
RV2000	100K Ohm	VRESLV	1
S1000	Button Function1	BUTTON	1
S1001, S1002	Button Function2	BUTTON	2
S1003	Button Function3	BUTTON	1
TE10	Test point PWM0	SIP-1	1
TE11	Test point PWM1	SIP-1	1
TE12	Test point PWM2	SIP-1	1
TE13	Test point PWM3	SIP-1	1
TE14	Test point PWM4	SIP-1	1
TE15	Test point PWM5	SIP-1	1
TE5022	PGND	SIP-1	1
TR2001	APC Transformer	TRAN-E133-2	1

Designator	Description	Footprint	Quantity
U13	TC4420	DIP8	2
U1000	MC74HC244	DIP20	1
U1001, U6002	LM293	DIP8	2
U1002	IRAMS10UP60A	IRAMS10UP60A-2	1
U2000	TOP223YAI	TO-220	1
U2001, U3001, U3002	NEC2501	DIP4	3
U2002	TL431	TL431	1
U3000	TC7660	SO-8	1
U3003	MAX202CSE	DIP16	1
U4000, U4001	74HC164	DIP14	2
U4002, U4003	FYQ-3641A	LG3641AH	2
U4004	MAX7219	DIP24	1
U5020	IR2125	DIP8	1
U5021	RELAY		1
U6001, U6003, U6004, U6005, U6006, U6007, U6008, U6010	MC33172	DIP8	8
U6009	REF196	DIP-8	1
VR2000	P6KE200	DIODE-0.4	1

INDEX

R

S

How to Reach Us:

Home Page:
www.freescale.com

E-mail:
support@freescale.com

USA/Europe or Locations Not Listed:
Freescale Semiconductor
Technical Information Center, CH370
1300 N. Alma School Road
Chandler, Arizona 85224
+1-800-521-6274 or +1-480-768-2130
support@freescale.com

Europe, Middle East, and Africa:
Freescale Halbleiter Deutschland GmbH
Technical Information Center
Schatzbogen 7
81829 Muenchen, Germany
+44 1296 380 456 (English)
+46 8 52200080 (English)
+49 89 92103 559 (German)
+33 1 69 35 48 48 (French)
support@freescale.com

Japan:
Freescale Semiconductor Japan Ltd.
Headquarters
ARCO Tower 15F
1-8-1, Shimo-Meguro, Meguro-ku,
Tokyo 153-0064, Japan
0120 191014 or +81 3 5437 9125
support.japan@freescale.com

Asia/Pacific:
Freescale Semiconductor Hong Kong Ltd.
Technical Information Center
2 Dai King Street
Tai Po Industrial Estate
Tai Po, N.T., Hong Kong
+800 2666 8080
support.asia@freescale.com

For Literature Requests Only:
Freescale Semiconductor Literature Distribution Center
P.O. Box 5405
Denver, Colorado 80217
1-800-441-2447 or 303-675-2140
Fax: 303-675-2150
LDCForFreescaleSemiconductor@hibbertgroup.com

DRM075
Rev. 1
10/2005